

# Efficient production of inhibitor-free foamy virus glycoprotein-containing retroviral vectors by proteoglycan-deficient packaging cells

Clara Marie Munz,<sup>1,4,9</sup> Henriette Kreher,<sup>1,9</sup> Alexander Erdbeer,<sup>1,5</sup> Stefanie Richter,<sup>1,2</sup> Dana Westphal,<sup>1,6</sup> Buqing Yi,<sup>1</sup> Rayk Behrendt,<sup>3,7</sup> Nicole Stanke,<sup>1,2</sup> Fabian Lindel,<sup>1,8</sup> and Dirk Lindemann<sup>1,2</sup>

<sup>1</sup>Institute of Medical Microbiology and Virology, University Hospital and Medical Faculty “Carl Gustav Carus”, Technische Universität Dresden, Fetscherstr. 74, 01307 Dresden, Germany; <sup>2</sup>Center for Regenerative Therapies Dresden (CRTD), Technische Universität Dresden, 01307 Dresden, Germany; <sup>3</sup>Institute of Immunology, Medical Faculty “Carl Gustav Carus”, Technische Universität Dresden, 01307 Dresden, Germany

**Foamy viruses (FVs) or heterologous retroviruses pseudotyped with FV glycoprotein enable transduction of a great variety of target tissues of disparate species. Specific cellular entry receptors responsible for this exceptionally broad tropism await their identification. Though, ubiquitously expressed heparan sulfate proteoglycan (HS-PG) is known to serve as an attachment factor of FV envelope (Env)-containing virus particles, greatly enhancing target cell permissiveness. Production of high-titer, FV Env-containing retroviral vectors is strongly dependent on the use of cationic polymer-based transfection reagents like polyethyleneimine (PEI). We identified packaging cell-surface HS-PG expression to be responsible for this requirement. Efficient release of FV Env-containing virus particles necessitates neutralization of HS-PG binding sites by PEI. Remarkably, remnants of PEI in FV Env-containing vector supernatants, which are not easily removable, negatively impact target cell transduction, in particular those of myeloid and lymphoid origin. To overcome this limitation for production of FV Env-containing retrovirus supernatants, we generated 293T-based packaging cell lines devoid of HS-PG by genome engineering. This enabled, for the first, time production of inhibitor-free, high-titer FV Env-containing virus supernatants by non-cationic polymer-mediated transfection. Depending on the type of virus, produced titers were 2- to 10-fold higher compared with those obtained by PEI transfection.**

## INTRODUCTION

Spuma- or foamy viruses (FVs) are a particular kind of retrovirus.<sup>1</sup> They constitute several genera in the retrovirus subfamily of the *Spumaretrovirinae* due to their unique replication strategy, which deviates in many aspects from that of all other retroviruses grouped into the *Orthoretrovirinae* subfamily.<sup>2,3</sup> One unique feature that distinguishes FVs from orthoretroviruses is their dependence of its cognate viral glycoprotein (GP) for budding and release of virions.<sup>4,5</sup> Unlike other retroviruses, the FV Gag protein lacks a membrane-targeting or -association domain.<sup>6,7</sup> Therefore Gag expression alone allows intracellular

formation of virus capsids following a B/D assembly strategy at the host cells' centrosome. However, the preassembled capsids are unable to associate to membranes or induce budding structures in the absence of FV GP coexpression.<sup>8</sup> This is because these processes depend on a very specific and direct interaction of the FV GP precursor cytoplasmic N terminus, which is the leader peptide (LP) domain, with the N terminus of the FV Gag protein.<sup>4,5,9,10</sup> Budding of many FV species (including simian FVs [SFVs] and feline FV [FFV]) appears to occur mainly at intracellular membranes, most likely representing Golgi compartments.<sup>6,8,11–13</sup> However, in addition, budding at the plasma membrane is observed for these FV species. Still other FV species (e.g. bovine FV [BFV] and equine FV [EFV]) appear to bud exclusively at the cell surface.<sup>14,15</sup> Their wide host range and tissue tropism is another special feature that is also associated with their GPs and makes FVs an interesting tool for gene-delivery systems for application in basic research and gene therapy.<sup>16,17</sup> Unfortunately, the responsible cellular entry receptor(s), which enable FV GP-mediated fusion and are essential for cytoplasmic access of the viral capsid, are largely

Received 30 October 2021; accepted 7 July 2022;

<https://doi.org/10.1016/j.omtm.2022.07.004>.

<sup>4</sup>Present address: Institute of Immunology, Medical Faculty “Carl Gustav Carus”, Technische Universität Dresden, 01307 Dresden, Germany

<sup>5</sup>Present address: Institut für Hydrobiologie, Technische Universität Dresden, 01062 Dresden, Germany

<sup>6</sup>Present address: Department of Dermatology, University Hospital “Carl Gustav Carus”, Technische Universität Dresden, 01307 Dresden, Germany

<sup>7</sup>Present address: Institut für Klinische Chemie und Klinische Pharmakologie, University Hospital Bonn, 53127 Bonn, Germany

<sup>8</sup>Present address: Cell Line Screening & Development (CLSD), Novartis Institutes for BioMedical Research (NIBR), 4056 Basel, Switzerland

<sup>9</sup>These authors contributed equally

**Correspondence:** Dirk Lindemann, Institute of Medical Microbiology and Virology, University Hospital and Medical Faculty “Carl Gustav Carus”, Technische Universität Dresden, Fetscherstr. 74, 01307 Dresden, Germany.  
**E-mail:** [dirk.lindemann@tu-dresden.de](mailto:dirk.lindemann@tu-dresden.de)

**Correspondence:** Fabian Lindel, Cell line Screening & Development (CLSD), Novartis Institutes for BioMedical Research (NIBR), WSJ-360, Kohlenstrasse, 4056 Basel, Switzerland.

**E-mail:** [fabian.lindel@novartis.com](mailto:fabian.lindel@novartis.com)



unknown. The only cellular factor identified so far that has a strong influence on FV infectivity is cell-surface heparan sulfate (HS).<sup>18–20</sup> Susceptibility of target cells toward FV GP-mediated infection positively correlates with their cell-surface HS proteoglycan (HS-PG) expression. Moreover, transduction of HS-deficient cells by FVs or FV GP pseudotyped retroviral vectors is reduced 20- to 50-fold,<sup>18,20</sup> though they are not completely resistant to FV GP-mediated transduction. Therefore, HS-PG is currently thought to function primarily as an attachment factor for FVs, facilitating the initial binding and thus increasing the concentration of virus particles on the cell surface. Thereby, subsequent interaction with specific, unknown entry receptors is enabled. In line with FV envelope (Env)-HS-PG interactions playing an important role in the early phases of FV replication is the observation that cationic polymers like polybrene or protamine sulfate, which are commonly used to enhance cell-free infection of many viruses, do not enhance or even slightly inhibit prototype FV (PFV) Env-mediated infection of target cells.<sup>21–26</sup>

Like chondroitin sulfate (CS) and dermatan sulfate (DS), HS is a glycosaminoglycan (GAG) that is covalently attached to core proteins that form PGs.<sup>27–29</sup> The polysaccharides of all GAGs, which are linear chains composed of different GAG-repeating disaccharide units, are attached to serine residues in core proteins through a common GAG-protein linkage tetrasaccharide. HS is composed of repeating units of uronic acid and glucosamine with variable additions of sulfate groups and other modifications. The high degree of sulfation confers a net negative charge, which allows for ionic interactions with cationic molecules of ligands. For example, HS is used as an attachment factor by a number of viruses, such as most herpes viruses, alpha viruses, human papilloma viruses, hepatitis C virus, adeno-associated virus, dengue virus, yellow fever virus, human respiratory syncytial virus, or vaccinia virus.<sup>28</sup> Furthermore, also cationic polymers, such as polyethyleneimine (PEI), cationic lipid mixtures, like lipofectamine, or cationic polypeptides, for example, polyarginine, bind to cell-surface HS.<sup>30–32</sup> Their interaction with HS is essential for their application as transfection reagents for delivery of various cargos, including nucleic acids or proteins, by endocytic uptake into target cells.

However, HS not only participates in attachment and uptake processes but also is an important cellular factor involved in the release of molecules and vesicular structures from cells. This includes a function of HS as a major regulator of release for several viruses. For example, herpes simplex virus (HSV), known to use HS as attachment factor for entry, in late phases of its replication induces an upregulation of cellular heparanase,<sup>33</sup> which is an endoglycosidase that degrades HS present at multiple cellular sites including the plasma membrane and extracellular matrix.<sup>34</sup> Thereby, cell-surface HS is almost completely removed in HSV-infected cells, which is essential for efficient release of HSV *in vitro* and tissue dissemination *in vivo*.

Whether HS also plays a role in the release of FVs or heterologous viral vector particles pseudotyped with FV GPs has so far not been

investigated, though some previous observations might indicate that they indeed do. For example, the titers of replication-deficient PFV vector supernatants generated by transient transfection of 293T packaging cells were found to be strongly dependent on the type of transfection reagent employed. Use of liposome-based<sup>35</sup> or calcium phosphate (CaP)<sup>36</sup> transfection techniques yielded much lower vector titers than cationic polymer-based reagents like activated dendrimers<sup>35</sup> or PEI,<sup>36</sup> known ligands of HS-PG.

The results of this study strongly suggest that the cationic polymers PEI and Polyfect enable the presence of high amounts of FV GP-containing virus or virus vector particles in the supernatant of virus- or virus vector-producing cells by neutralizing interaction of the particles with cellular HS-PG of the virus- or virus vector-producing cell. Furthermore, we demonstrate that cationic polymers are efficient inhibitors of FV GP-mediated virus or viral vector uptake. We also found that remnants of the cationic polymers present in the cell-free virus supernatants, which are not easily removable by post-harvest purification methods, interfere with infection or transduction of lymphoid and myeloid target cells. Generation of PG-deficient packaging cells alleviated the need for cationic polymer-based transfection reagents for production of inhibitor-free, high titer FV GP-containing retroviral vector supernatant by enabling the use of CaP transfection methodology.

## RESULTS

### Unusual titration phenotype of PEI-derived FV Env-containing vector supernatants on THP-1 cells

Replication of FVs *in vitro* is characterized by very strong cytopathic effects ultimately leading to the death of most target cell types. The only cell types known that allow establishment of persistent infections by replication-competent FVs are of lymphoid or myeloid origin.<sup>17,37,38</sup> When we titrated various replication-deficient, single-round retroviral vector (SRV) supernatants, based on lentivirus (human immunodeficiency virus type 1 [HIV]), gamma retrovirus (Moloney murine leukemia virus [MLV]), or prototype FV (PFV) origin on the human myeloid cell line THP-1, we observed a unique titration phenotype that positively correlated with the presence of FV GPs (PFV Env [PE]; macaque sFV Env [SE]) in the respective vector particles of different retroviral origin (Figures 1A and S1A). This phenotype was characterized by a low transduction efficiency at high vector doses. A subsequent reduction of the vector dose by dilution of vector supernatants led to the unusual observation that the transduction efficiency stayed constant or even increased until a maximum was reached. Only a further reduction of the vector dose led again to a decline of the transduction efficiency. Titration of the identical vector supernatants, generated by transient transfection of 293T packaging cells using different cationic polymers (PEI; Polyfect), on HT1080 fibrosarcoma cells did not reveal this phenotype (Figures 1B and S1B). Here, a dose-dependent decline of the transduction efficiency was observed when the virus dose was reduced by serial dilution of vector supernatants. In contrast, retroviral vectors pseudotyped with VSV-G (HIV-VSV; MLV-VSV) did not show this conspicuous phenotype on THP-1 cells, as a dose-dependent reduction of the

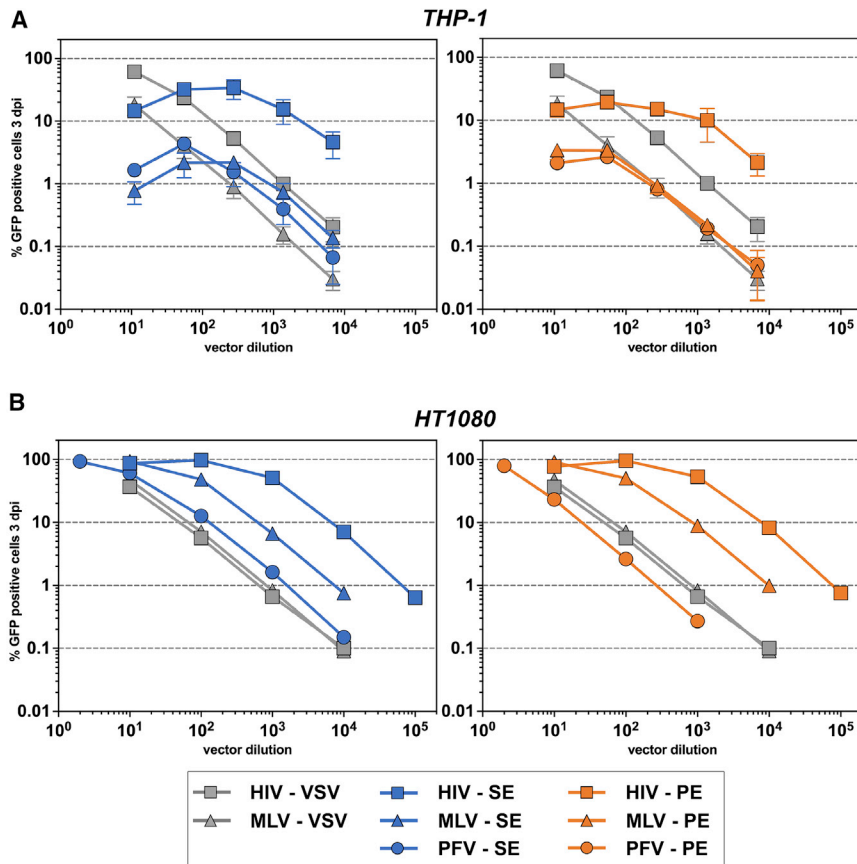


**Figure 1. Differential susceptibility of human epithelial and monocytic cell lines toward FV Env-containing single-round retrovirus vector particles**

GFP-expressing retroviral vector supernatants of PFV, HIV, or MLV origin pseudotyped with different viral GPs (PFV Env [PE], SFVmac Env [SE], or VSV-G [VSV]), as indicated, were generated using wild-type 293T packaging cells, and PEI transfection methodology as described in materials and methods. (A and B) THP-1 (A) and HT1080 (B) target cells were incubated with decreasing serial dilutions of the identical, plain, cell-free vector supernatants pseudotyped with the respective GP as indicated. Three days post-infection (dpi), the percentage of GFP-expressing cells in the individual samples was determined by flow cytometry. Shown are the mean  $\pm$  SD of three independent titrations on THP-1 cells of separate aliquots of the same vector supernatant production and a single titration on HT1080 cells.

mock supernatant with plasmid DNA (293T + DNA) did not alter its THP-1 transduction phenotype (Figure S2A). In contrast, addition of mock supernatant with PEI (293T + PEI) or with PEI and DNA (293T + PEI-DNA) did prevent the initial increase of the transduction efficiency observed for the first serial dilutions of HIV-SE supernatant, with the former mock supernatant having a stronger inhibitory effect. In contrast, no changes in transduction efficiencies on THP-1 cells were observed when taking any of the mock supernatants as diluent for LV pseudotyped with VSV-G (HIV-VSV) (Figure S2B). This strongly indicated that PEI is the putative FV Env-specific inhibitory factor.

transduction efficiency was observed on both THP-1 and HT1080 cells upon serial dilution of vector supernatants (Figures 1 and S1).

#### PEI is the inhibitory factor of the FV Env-dependent transduction phenotype

To identify the underlying reason for this FV GP-dependent transduction phenotype, we pursued several avenues. One hypothesis examined was that our vector supernatant contains a factor that specifically inhibits FV GP-mediated transduction of THP-1 cells. The inhibitory activity of this factor would be reduced by serial dilutions of vector supernatant, resulting in an enhanced transduction efficiency until its concentration declines below biological function. This hypothesis was tested by titration of lentiviral (LV) vector supernatants either containing SFVmac Env (HIV-SE) or VSV-G (HIV-VSV) GPs using not only standard growth medium (medium) as diluent but also various mock supernatants derived from 293T cells treated in different ways (Figure S2). The mock supernatants were generated analogous to retroviral vector supernatants by transient transfection except that one or both components (PEI and non-viral DNA) were omitted during the procedure. Equal volumes of serial dilutions of cell-free supernatants of LV pseudotyped with SFVmac Env (HIV-SE) or VSV-G (HIV-VSV) and undiluted mock supernatants were mixed prior to addition to THP-1 target cells. Serial dilutions of HIV-SE supernatants mixed with a constant amount of normal mock supernatant (293T) or

#### The FV Env-dependent transduction phenotype is influenced by the amount of PEI and the presence of cell-surface HS

A rough estimate of the residual PEI amount in the virus supernatant can be calculated. Taking into account the initial concentration of PEI used for transfection (8  $\mu$ g/mL) and assuming its homogeneous distribution in the liquid phase as well as an up to 10% carryover of liquids during the two media change steps of the viral vector production procedure, the harvested, cell-free, plain retroviral vector supernatants may contain about 56 ng/mL residual PEI. The data from the analysis of PEI mock supernatants (293T + PEI) suggested that only at dilutions of 1:300 or higher was a dose-dependent reduction of the transduction efficiency observed for supernatants of LV pseudotyped with SFVmac Env (HIV-SE), and the difference between mock (medium) and PEI mock (293T + PEI) diluent treated sample transduction efficiencies stayed constant (Figure S2A). Taken together, this indicates that the inhibition of SFVmac Env-mediated transduction of THP-1 cells requires concentrations of PEI of at least 0.2 ng/mL.

With these thoughts in mind, we evaluated the influence of adding exogenous PEI, at defined doses of 0.5–312.5 ng/mL, to supernatants

of LV pseudotyped with either SFVmac Env (HIV-SE) or VSV-G (HIV-VSV) on their transduction efficiency of THP-1 and other suspension or adherent target cell lines (Figure 2). The transduction efficiency of THP-1 and Jurkat cells by HIV-VSV (Figures 2A and 2B) was not affected by PEI at any of the concentrations examined, whereas its transduction efficiency of HT1080 or L929 cells (Figures 2C and 2D) was enhanced up to 2.2- and 3.3-fold, respectively, at the highest PEI concentration tested. Interestingly, this enhancement was not observed for Sog9 fibroblasts (Figure 2E), which are an HS-deficient variant of L929 parental cells<sup>39</sup> (Figure S3A). In contrast, a dose-dependent, PEI-mediated inhibition of the transduction efficiency of HIV-SE was observed for THP-1, Jurkat, HT1080, and L929 cells (Figures 2A–2D). For the THP-1 and Jurkat suspension cells, PEI at its highest concentration of 312.5 ng/mL inhibited transduction up to 40-fold, and PEI concentrations as low as 2.5 ng/mL did show a significant inhibitory effect (Figures 2A and 2B). For HT1080 and L929 adherent cells, an inhibition was observed only at the two highest PEI concentrations examined (62.5 and 312.5 ng/mL), and the maximal inhibition was lower (4-fold) than on suspension cells (Figures 2C and 2D). Strikingly, even the highest PEI concentration examined did not alter SFVmac GP-mediated transduction of HS-deficient Sog9 adherent cells (Figure 2E). These results further support a role for remnants of the transfection reagent PEI as inhibitor of FV GP-mediated transduction for certain target cell types. Furthermore, the results suggest that target cell-surface HS expression plays an important role for PEI-mediated inhibition of FV Env containing retroviral vector transduction efficiency.

#### Purification methods to remove remnants of PEI from virus supernatants

We examined various additional post-production purification procedures on FV Env-containing retroviral vector supernatants for their potential to overcome/remove the PEI-mediated inhibitory activity (Figure S4). However, neither particle purification and concentration by ultracentrifugation (UC), a combination of UC followed by ultrafiltration (UC + UF), nor size-exclusion chromatography (SEC) purification, result in a complete neutralization of the inhibitory effect observed for plain (P) supernatants of LV pseudotyped with SFVmac Env (Figure S4A). Only the latter two methods did appear to have a somewhat beneficial effect, indicated by an earlier linear correlation of supernatant dose and percentage of GFP-positive cells upon serial dilution of vector supernatant, though all of them appear to reduce vector yield 2- to 4-fold.

#### Cationic polymers improve the cell-free, physical titer of FV Env-containing virus particles produced by HS-PG-expressing packaging cells

We<sup>36</sup> and others<sup>35</sup> have previously observed that the titers of replication-deficient PFV vectors or retroviral vectors pseudotyped with FV GPs produced by transient transfection of 293T cells are significantly influenced by the type of transfection reagent used. The use of cationic polymers like PEI (unpublished data) or dendrimers, such as Polyfect,<sup>35,36</sup> resulted in titers of vector particle naturally released into the supernatants of packaging cells that are 10- to 100-fold higher than those of other transfection reagents like CaP (Figure S5A) or li-

posomes.<sup>35</sup> In contrast, artificial release of vector particles by freeze thawing of packaging cells prior to harvest of cell-free vector supernatants resulted in similar vector titers for all transfection reagents used (Figure S5A). Western blot analysis of cellular viral protein expression and viral particle release indicated that cell-free, physical particle amounts in supernatants of CaP-transfected packaging cells is strongly reduced, although cellular expression levels were similar or even higher compared with Polyfect-transfected cells (Figure S5B). Therefore, we hypothesized that cationic polymer-based transfection reagents might neutralize unknown factor(s) on wild-type 293T cells that otherwise retain FV GP-containing retroviral particles at the surface of cells (Figures S6A and S6B). FV GP-containing retroviral particles have been reported to use cell-surface HS as an attachment factor during adsorption and entry into target cells.<sup>19,20</sup> Furthermore, cationic polymers like PEI are known to also bind to GAGs and HS in particular.<sup>32</sup> Therefore, we reasoned that HS on the cell surface of 293T cells is the or is one of the unknown factor(s) neutralized by cationic polymer-based transfection reagents, enabling the presence of high numbers of FV GP-containing retroviral vector in the supernatant of packaging cells.

To examine the role of packaging cell HS expression on physical and biological FV particle titers, we generated 293T packaging cells lacking HS by CRISPR-mediated inactivation of a key enzyme of PG biosynthesis, beta-1,3-glucuronyltransferase 3, encoded by the *B3GAT3* gene. By inactivation of *B3GAT3*, all GAG chains of PGs terminate after the third residue of the common GAG-protein linker region tetrasaccharide, resulting in packaging cells devoid of functional HS-, CS-, and DS-PG.<sup>40</sup> Two independent clonal cell lines, 293T-25A and 293T-306, out of 23 total that were negative in flow cytometry analysis after HS cell-surface staining (Figure S3B) were characterized in greater detail.

First, we examined their capacity to support retroviral vector production employing different viral GPs and transfection methodologies and compared it with parental wild-type 293T packaging cells (Figures 3 and S7). Various combinations of packaging and GFP-expressing transfer vector plasmids for production of replication-deficient SRV particles based on PFV, MLV, or HIV were transfected into wild-type (WT) 293T cells or the PG-deficient variants 293T-25A (25A) and 293T-306 (306) using either CaP or PEI methodologies. Titration of vector supernatants on HT1080 cells demonstrated a 20- to 60-fold increase in vector titers for PFV SRVs harboring PFV (PFV-PE) or SFVmac Env (PFV-SE) proteins produced by CaP transfection using 293T-25A or 293T-306 cells compared with the parental 293T cells (Figures 3B and 3C). PFV SRV titers of plain, cell-free 293T-25A or -306 supernatants, derived from CaP transfections, were at a similar level ( $10^6$  enhanced green fluorescent protein [EGFP] TU/mL) as the titers obtained by PEI transfection of any of the three 293T variants (Figure 3A). For LV SRV pseudotyped with FV Envs (HIV-PE, HIV-SE) and produced by CaP transfection, the use of 293T-25A or -306 cells resulted in titers of  $0.5\text{--}1.0 \times 10^8$  EGFP TU/mL for plain cell-free cell culture supernatants, which were 2- to 3-fold higher than those obtained with WT 293T cells



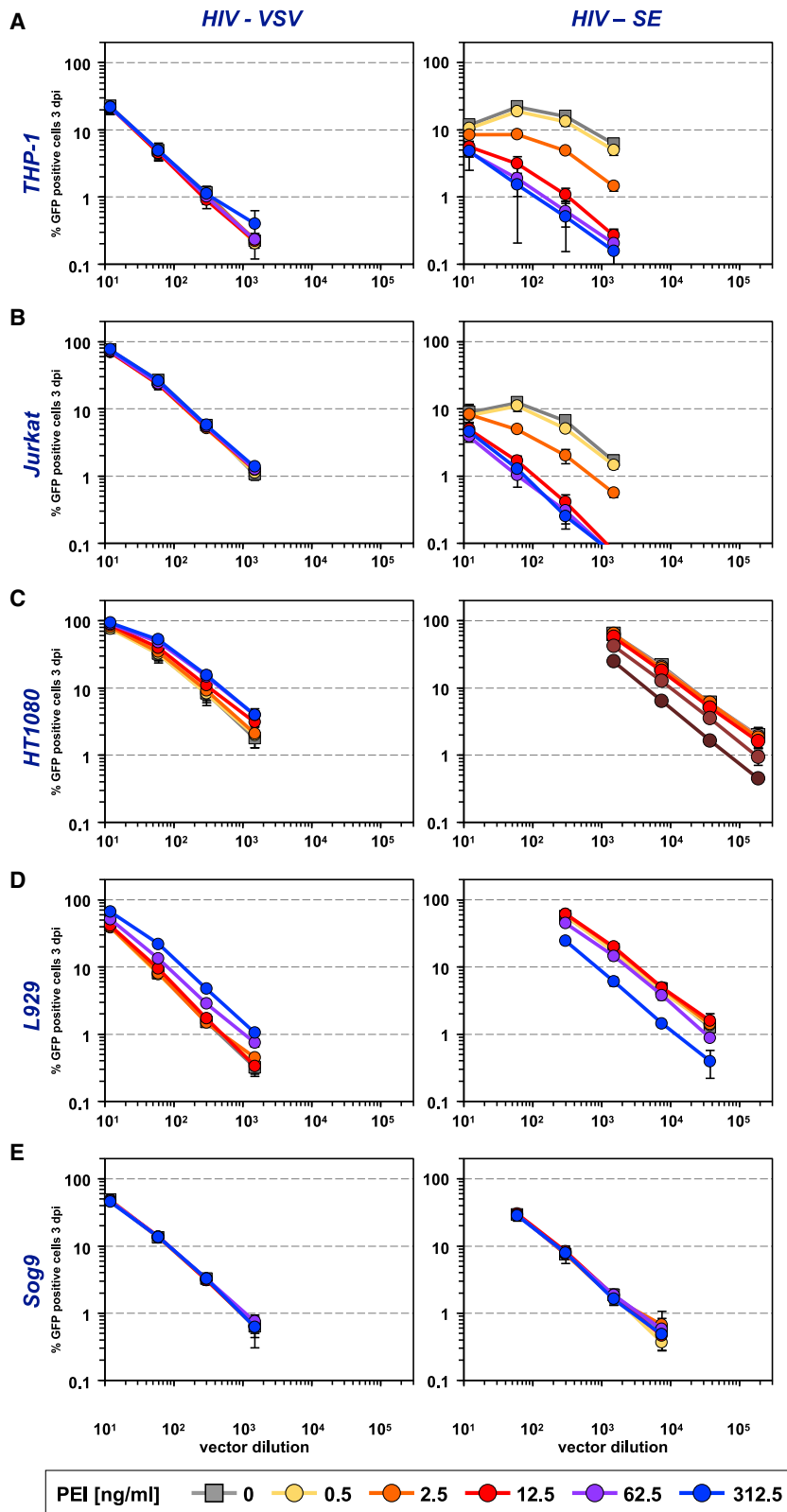
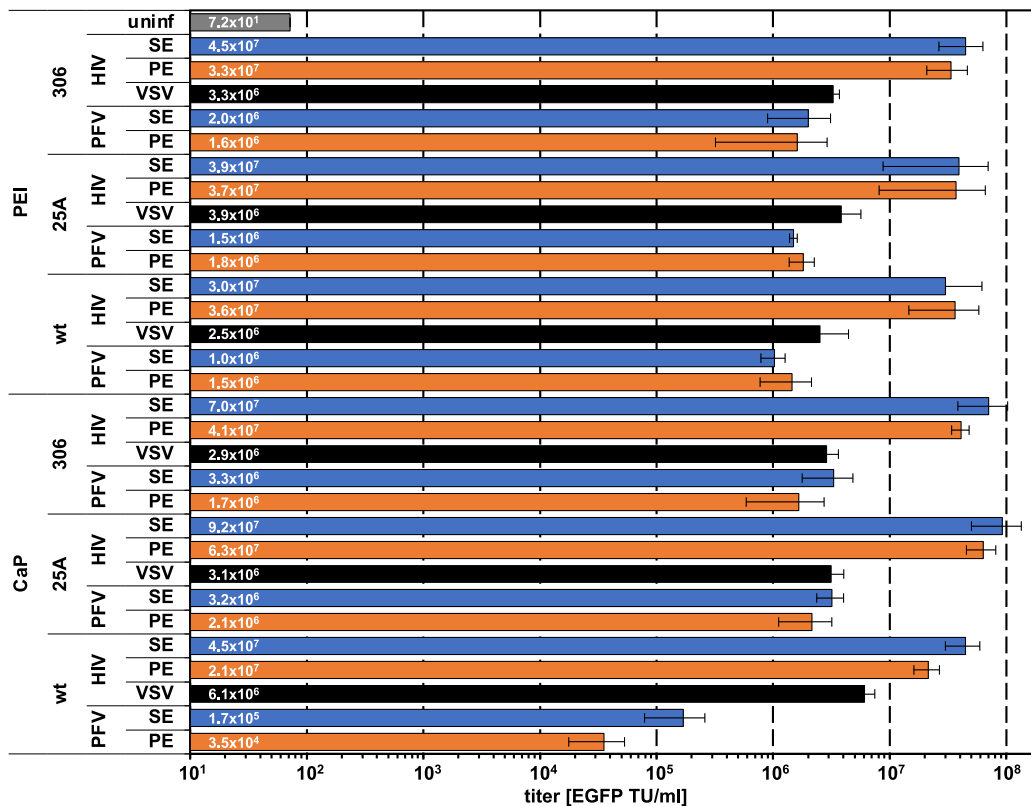


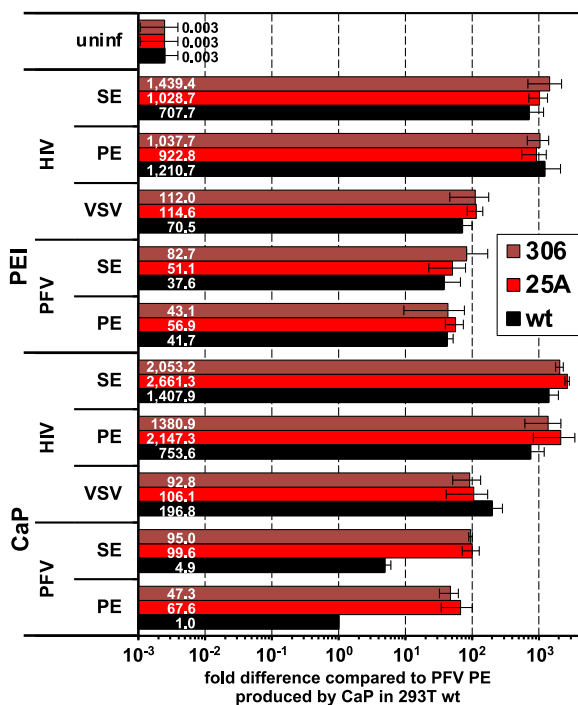
**Figure 2. Viral glycoprotein-dependent influence of exogenous PEI addition on retroviral vector transduction efficiency of different target cells**

GFP-expressing LV vector supernatants pseudotyped with VSV-G (HIV-VSV) or SFVmac Env (HIV-SE) were generated using wild-type 293T packaging cells and PEI transfection methodology, as described in [materials and methods](#). (A–E) Different target cells of (A) myeloid, (B) lymphoid, or (C–E) fibroblast origin, as indicated, were incubated with decreasing serial dilutions of the identical LV supernatants, pseudotyped with the respective GP, as indicated, that contained fixed concentrations of exogenously added PEI, as indicated. Shown are the mean  $\pm$  SD ( $n = 3$ ) of the percentage of GFP-expressing cells in the individual samples determined 3 dpi by flow cytometry.

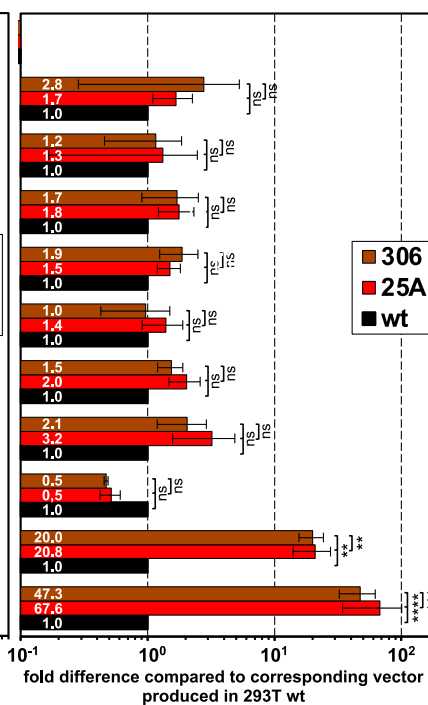
A



B



C



(legend on next page)

(Figures 3B and 3C). In contrast, titers of LV SRV pseudotyped with VSV-G (HIV-VSV) obtained by using 293T-25A or -306 cells and CaP transfection were 2-fold reduced compared with 293T WT cells, though both changes were not statistically significant. When using the PEI transfection method, no major influence of the packaging cell type employed on the vector titer was observed for the different vector combinations (Figure 3).

#### The absence of PGs results in high amounts of FV GP-containing vector particles

Next, we examined whether the strongly increased vector titer of PFV SRV supernatants achieved by CaP-mediated transient transfection of PG-deficient 293T-25A cells also applies to other types of PFV expression systems. Furthermore, we intended to determine whether the titer increase is due to an enhanced physical particle number in the supernatants or is the result of an increased specific particle infectivity. Expression plasmids for production of replication-deficient, standard PFV SRV or non-viral RNA-transfer vectors (TraFo) as well as replication-competent PFV (RCV) were transfected into 293T WT or -25A cells using either CaP or PEI methodologies (Figures 4, 5, and S7). Cell-free vector or virus supernatants were titrated on different target cells as well as cellular FV protein expression, and FV particle protein composition was determined by western blot analysis. For all three PFV particle types, western blot analysis of concentrated vector or virus particle samples revealed that CaP-transfected, PG-deficient 293T-25A cells allowed a much higher physical particle release than CaP-transfected, parental 293T WT cells (Figures 4 and 5A). The most dramatic increase (>27-fold) in physical particle release was observed for RCV supernatants obtained by transfection of full-length proviral expression constructs into 293T-25A cells using CaP methodology (Figures 4, lanes 9 and 15, and 5A). Strikingly, physical, but also biological, titers of RCV supernatants obtained by CaP transfection of 293T-25A cells were superior to that of either 293T WT or 293T-25A packaging cells employing PEI methodology (Figures 5A and 5B). Interestingly, CaP-25A-derived RCV particles displayed an enhanced Gag precursor processing, which correlated with the presence of a higher amount of particle-associated mature Pol p85<sup>PR-RT</sup> and p40<sup>IN</sup> subunits than in PEI-25A or PEI-WT-derived RCV virions (Figure 5A). The relative ratios of precursor and processed PFV Gag found in PFV particles are known to strongly influence

their biological activity.<sup>41–43</sup> Therefore, the up to 10-fold higher infectious titers of CaP-25A PFV RCV supernatants compared with PEI-25A or PEI-WT PFV RCV supernatants (Figure 5B) are most probably the consequence of combination of an increase in both physical particle release and specific particle infectivity.

#### PG-deficient packaging cells are less permissive for and resistant to PEI-mediated inhibition of FV GP mediated transduction

Next, we compared the susceptibility of parental, WT, and *B3GAT3*-deficient 293T cells toward FV GP-mediated transduction by different retroviral vectors (Figure 6). Transductions with serial dilutions of SRV supernatants revealed a minor (2-fold) reduction in permissiveness of 293T-25A or -306 cells toward LV vectors pseudotyped with VSV-G (HIV-VSV). In contrast, transduction of 293T-25A or -306 cells by LV vectors pseudotyped with PFV (HIV-PE) or SFVmac Env (HIV-SE) or PFV SRVs harboring PFV (PFV-PE) or SFVmac Env (PFV-SE) proteins was reduced 50- to 100-fold compared with WT 293T cells. These results are in line with previous reports<sup>18–20</sup> and support the importance of HS-PG for FV GP-mediated target cell transduction.

In addition, we reexamined the potential inhibitory effect of PEI remnants in retroviral vector supernatants on FV GP-mediated transduction using this set or 293T cell variants. First, we used serial dilutions of PEI-free LV vector supernatants, produced by CaP transfection and carrying different viral GPs, to transduce WT 293T (293T-WT) and HS-deficient 293T-25A (293T-25A) target cells in the absence or presence of various amounts of exogenously added PEI (Figure 7). Due to the reduced permissiveness of 293T-25A cells to FV GP-mediated transduction compared with 293T-WT cells, higher amounts of HIV-PE or HIV-SE supernatants were necessary to achieve similar levels of GFP-reporter-expressing cells (Figures 6 and 7). The analysis confirmed the earlier observation (Figure 2) that the transduction of LV vectors pseudotyped with VSV-G (HIV-VSV) was not inhibited by PEI addition on both target cell types (Figure 7A). A moderate (3-fold) enhancement of the transduction efficiency of HIV-VSV was observed for both target cell types at the highest PEI concentration used. In contrast, as seen before (Figure 2), the transduction efficiency of HIV-PE and HIV-SE on 293T-WT, but not PG-deficient 293T-25A, cells was inhibited in a dose-dependent manner (Figures 7B and 7C). A clear inhibition of

#### Figure 3. Comparison of PFV and LV vector titers obtained by transient transfection of various 293T packaging cell lines

Parental 293T (wild-type [WT]) or PG-deficient 293T variant (25A, 306) packaging cell lines were transiently transfected with expression plasmids encoding for either a replication-deficient, expression optimized 4-component PFV (PFV) vector system or a replication-deficient 3-component LV (HIV) vector system using PEI or CaP transfection reagents. GP packaging plasmids employed encoded PFV Env protein (PE, orange bars), macaque SFV Env protein (SE, blue bars), or the VSV glycoprotein (VSV, black bars). Subsequently, infectivity of supernatants was determined by titration on HT1080 target cells using a flow cytometric EGFP transfer assay. (A) Mean values  $\pm$  SD ( $n = 3$ ) of absolute vector titers of plain supernatants on HT1080 target cells are shown. (B and C) The infectivity data of (A) are regrouped so that for each vector type, the infectivity obtained by production in 293T WT (black bars), 25A (bright red bars), or 306 (dark red bars) packaging cells are compared with each other. (B) Mean values  $\pm$  SD of fold difference of vector titers of individual samples relative to PFV vector supernatants containing PFV Env and derived by CaP-mediated transient transfection of parental 293T (WT) packaging cells are shown. (C) Mean values  $\pm$  SD of fold difference of vector titers of the individual samples, grouped by vector type, relative to the respective type of vector derived by transient transfection of parental 293T (WT) packaging cells. For each vector type, the respective vector titer obtained by transfection of 293T WT packaging cells was set as reference to 1, and the vector titers obtained by transfection of 293T-25A or -306 packaging cells are expressed as relative values to the respective reference. Two-way ANOVA with Tukey's multiple-comparisons test was used to assess significance. \*  $p < 0.05$ ; \*\*  $p < 0.01$ ; \*\*\*  $p < 0.001$ ; \*\*\*\*  $p < 0.0001$ ; ns: not significant ( $p \geq 0.05$ ).

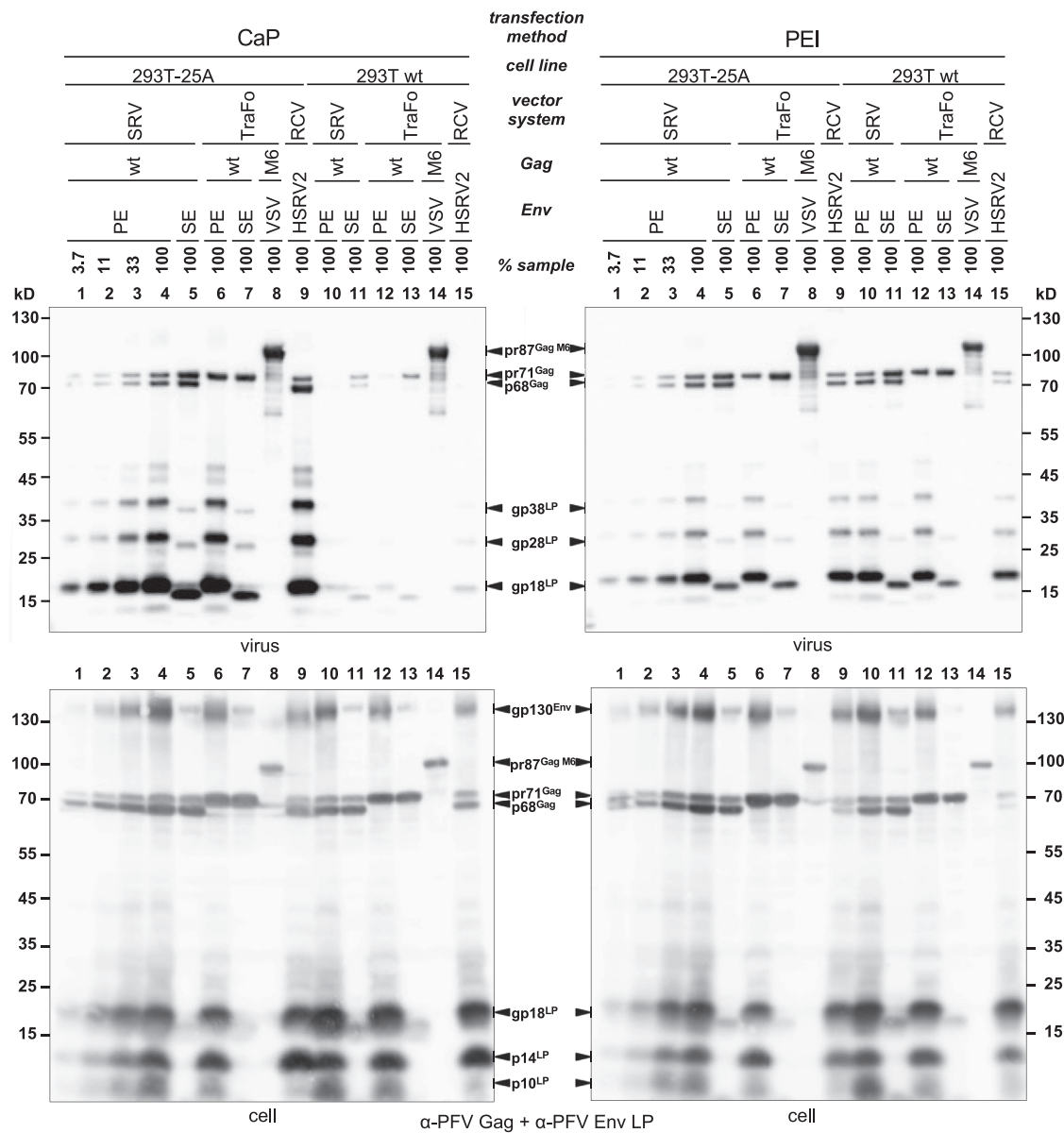


**Figure 4. Comparison of physical particle release obtained by transient transfection of various 293T-based packaging cell lines with components of different FV vector systems**

Parental 293T (WT) or PG-deficient 293T variant (25A) packaging cell lines were transiently transfected with PFV proviral expression constructs for production of replication-competent PFV (RCV) or expression constructs for production of EGFP encoding replication-deficient PFV single-round vector particles (SRVs) or expression constructs for production of EGFP encoding replication-deficient PFV RNA-transfer vector particles (TraFo) harboring PE, SE, or VSV as indicated, using PEI or CaP transfection methodologies. Physical particle release was determined by western blot analysis of equal volumes (100% sample) of samples of PFV particles concentrated and purified by ultracentrifugation followed by SDS-PAGE and immunoblotting using PFV Gag and PFV Env LP subunit-specific polyclonal antisera. A 3-fold serial dilution of the PFV SRV PE sample is shown in lanes 1 to 4. Shown are data from a representative experiment (n = 2). The infectivity data of the respective viral supernatants are shown in [Figure S8](#).

293T-WT target cell transduction was detectable by as little as 12.5 ng/mL PEI and was reduced by more than 10-fold at the highest PEI concentration used. This supports our earlier notion that cationic polymers like PEI inhibit attachment of FV GP-containing particles to HS-PG on the surface of target cells ([Figure S6](#)).

**CaP-derived FV GP-containing retroviral vector supernatants display enhanced transduction capacity of myeloid target cells**

Finally, to confirm that the unusual titration phenotype of FV GP-containing retroviral vectors observed on lymphoid or myeloid target cells is indeed the result of PEI remnants being



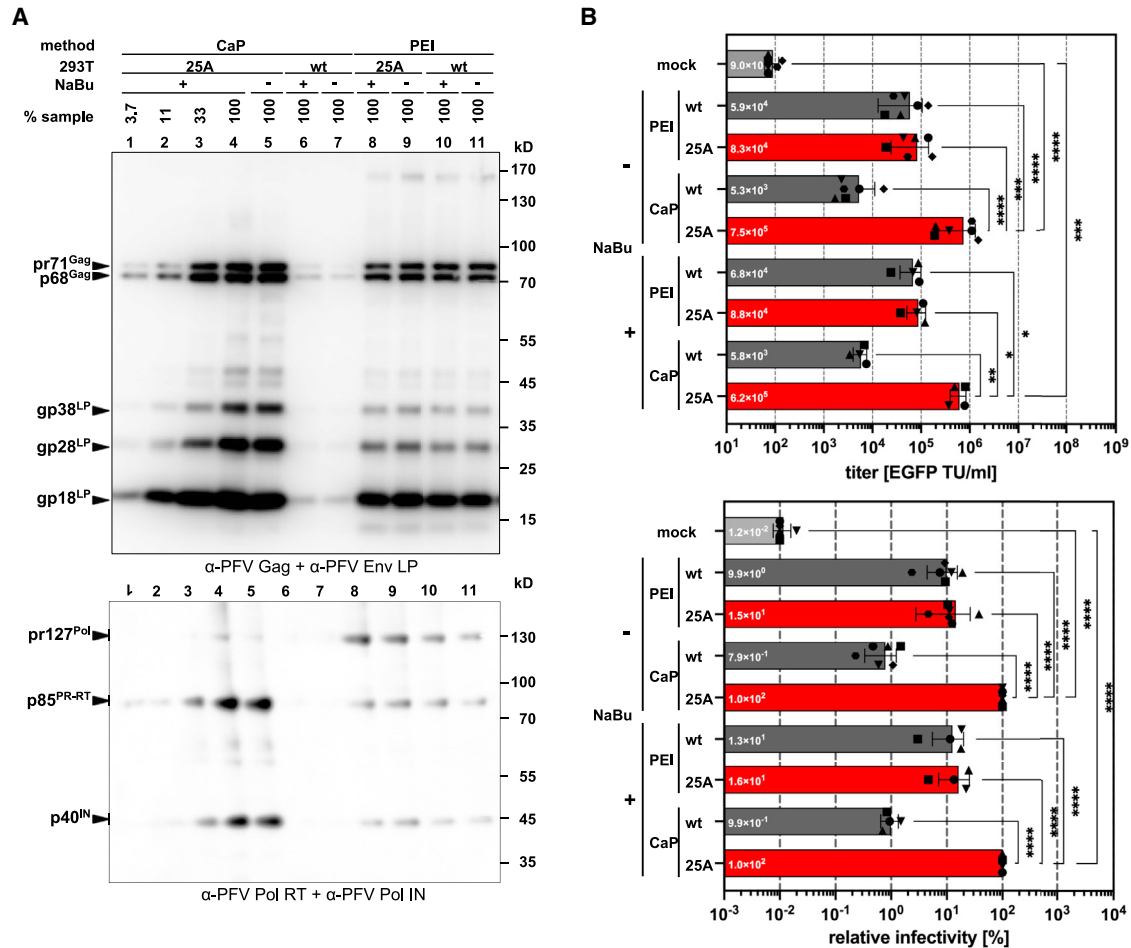


**Figure 5. Comparison of replication-competent PFV titers and physical particle release obtained by transient transfection of various 293T-based packaging cell lines**

Parental 293T (WT) or PG-deficient 293T variant (25A) packaging cell lines were transiently transfected with PFV proviral expression constructs using PEI or CaP transfection methods with (+) or without (–) sodium butyrate (NaBu) induction. (A) Physical particle release was determined by western blot analysis of equal volumes (100% sample) of samples of PFV particles concentrated and purified by ultracentrifugation followed by SDS-PAGE and immunoblotting using PFV Gag and PFV Env LP subunit-specific polyclonal antisera. A 3-fold serial dilution of the CaP 25A sample is shown in lanes 1 to 4. (B) Infectivity of supernatants was determined on HT1080 PLNE target cells harboring a PFV transactivator Tas-dependent EGFP reporter protein expression cassette using a flow cytometric assay at 24 h post-infection (hpi). Mean values  $\pm$  SD ( $n = 4–6$ ) of absolute viral titers on HT1080 PLNE target cells as well as relative infectivity in comparison to virus supernatants produced by CaP-mediated transient transfection of PG-deficient 293T-25A (25A) packaging cells are shown. Two-way ANOVA with Tukey's multiple-comparisons test was used to assess significance. \*  $p < 0.05$ ; \*\*  $p < 0.01$ ; \*\*\*  $p < 0.001$ ; \*\*\*\*  $p < 0.0001$ ; ns: not significant ( $p \geq 0.05$ ).

present, we titrated PFV- and LV-SRV supernatants produced by either PEI or CaP transfection on THP-1 target cells (Figures 8, S8A, and S8B). The unusual titration phenotype, characterized by equal or lower non-saturating transduction efficiencies at higher virus amounts, was reproducible for titrations on THP-1 cells using PEI-derived FV GP-containing, but not VSV-G-containing, vector supernatants. In contrast, this effect was almost completely alleviated for CaP-derived FV GP-containing supernatants, though at higher viruses doses, the dose-response curve of LV pseudotyped with VSV-G (HIV-VSV) had a steeper slope than those pseudotyped with FV GPs (HIV-PE, HIV-SE) (Table S3).

These results provide additional evidence for transfection reagent remnants of PEI-derived retroviral vector supernatants being the factor inhibition myeloid and lymphoid target cell transduction by FV GP-containing vector particles. Furthermore, this observation shows that by using CaP transfection of PG-deficient 293T-25A or -306 cells not only higher titers of FV Env-containing particles can be obtained in comparison to parental, 293T-WT cells but also higher transduction efficiencies of myeloid and lymphoid target cells will be achieved.

## DISCUSSION

Cell-surface HS-PG was previously identified as a crucial attachment factor for PFV and FFV, whereas other PGs did not seem to be

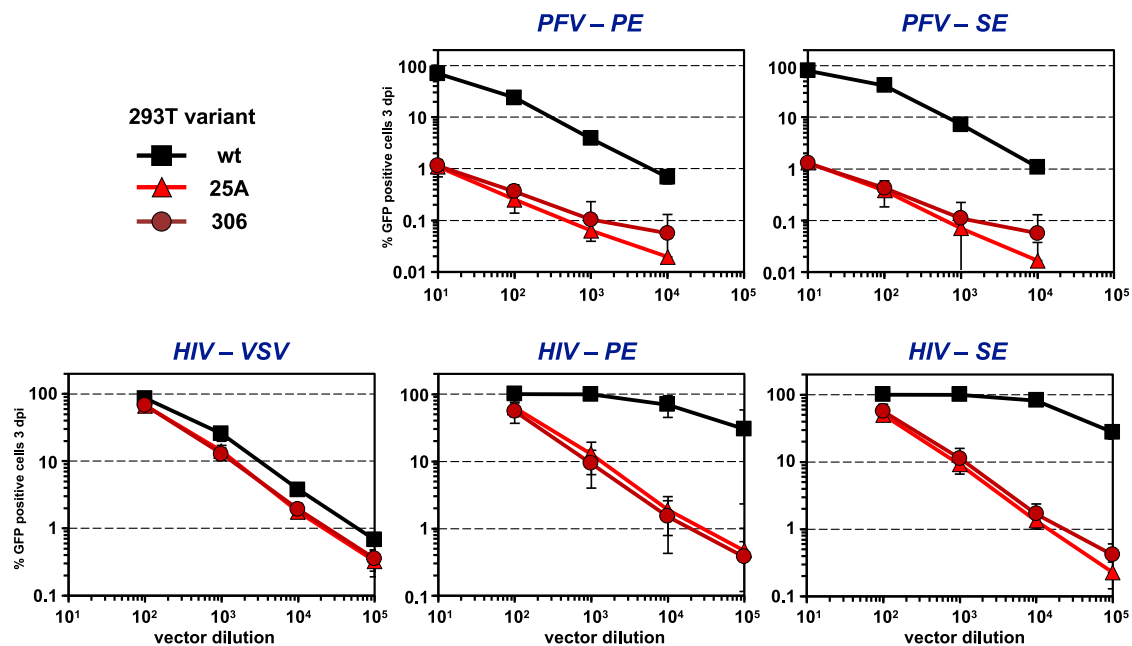


**Figure 6. Reduced permissiveness of PG-deficient 293T cells toward FV GP-containing retroviral vector particles**

Wildtype 293T cells (WT) or PG-deficient variants (25A, 306) were incubated with decreasing serial dilutions of GFP-expressing PFV (PFV) or LV (HIV) vector particles harboring VSV-G (VSV), PFV (PE), or SFVmac (SE) glycoproteins, as indicated. PFV and LV vector supernatants were generated by transient transfection of 293T-25A packaging cells using CaP transfection method. Three dpi, the percentage of GFP-expressing cells in the individual samples was determined by flow cytometry. Shown are the mean values  $\pm$  SD ( $n = 3$ ) of the percentage of GFP-expressing cells.

involved in FV Env-mediated virus uptake.<sup>19,20</sup> Whether HS-virus interactions are also relevant for late phases in the FV replication cycle, in particular viral egress, was not investigated previously. The results of our study suggest, for the first time, that they indeed do, by negatively influencing the levels of cell-free virions in the supernatant. However, whether HS-PG on the surface of the virus-producing cell prevents efficient virion release in the first place or, alternatively, enables immediate efficient reattachment and adsorption of released FV Env-containing particles after initial release cannot be distinguished from our experiments.

Cell-free viral titers of RCV PFV, single-round PFV, or orthoretroviral vectors harboring various FV GPs (PFV, SFVmcy, SFVggo) produced in PG-deficient 293T-25A or -306 packaging cells using CaP transfection methodologies were enhanced 1.5- to 100-fold relative to using 293T-WT cells. In contrast, the titers achieved for the individual types of virus supernatant by using the different packaging cells in combination with PEI transfection varied only slightly, up to 3-fold. Titers of CaP-derived orthoretroviral vectors pseudotyped with FV GPs increased only slightly ( $\sim$ 1.5- to 3-fold), and it is not clear whether this is due to an enhanced physical particle release or GP incorporation, as it was not investigated in detail. In contrast, the titer increase for PFV-based SRVs was much more pronounced ( $\sim$ 20- to 70-fold) and highest for PFV RCVs derived from PFV proviral expression constructs (up to 100-fold). In the case of PFV supernatants, the titer increase appears to be largely the result

of the presence of higher physical particle numbers in the cell-free supernatants. It can be speculated that the GP dependency of FV budding and particle release<sup>4,6</sup> might be responsible for the more pronounced infectious and physical virus titers achieved by using PG-deficient packaging cells. However, the subcellular location of virus budding, in the case of orthoretrovirus vectors pseudotyped with heterologous GPs at the plasma membrane and for PFV largely at intracellular compartments and only to some extent at the plasma membrane, may influence the effect of PG expression on viral titers.

In general, the virus titers achieved by CaP transfection using PG-deficient 293T packaging cells were similar to those obtained by PEI transfection using either PG-deficient or 293T-WT packaging cells. This was true for orthoretroviral vectors pseudotyped with FV GPs and PFV SRVs but not PFV RCVs. For the latter, up to 10-fold higher titers could be achieved by using CaP transfection in combination with PG-deficient 293T packaging cells, which can only be partially explained by higher physical particle numbers. Strikingly, the CaP- and 293T-25A-derived PFV RCVs consistently showed an enhanced Gag processing. This resulted in virions containing more p68<sup>Gag</sup> than pr71<sup>Gag</sup>, which was different for PFV RCVs produced by PEI transfection on either WT or 293T-25A packaging cells. Such virions contained roughly equal amounts of pr71<sup>Gag</sup> and p68<sup>Gag</sup>. As it is known that the pr71<sup>Gag</sup> and p68<sup>Gag</sup> ratio influences PFV infectivity<sup>41-43</sup> this difference might account for the further

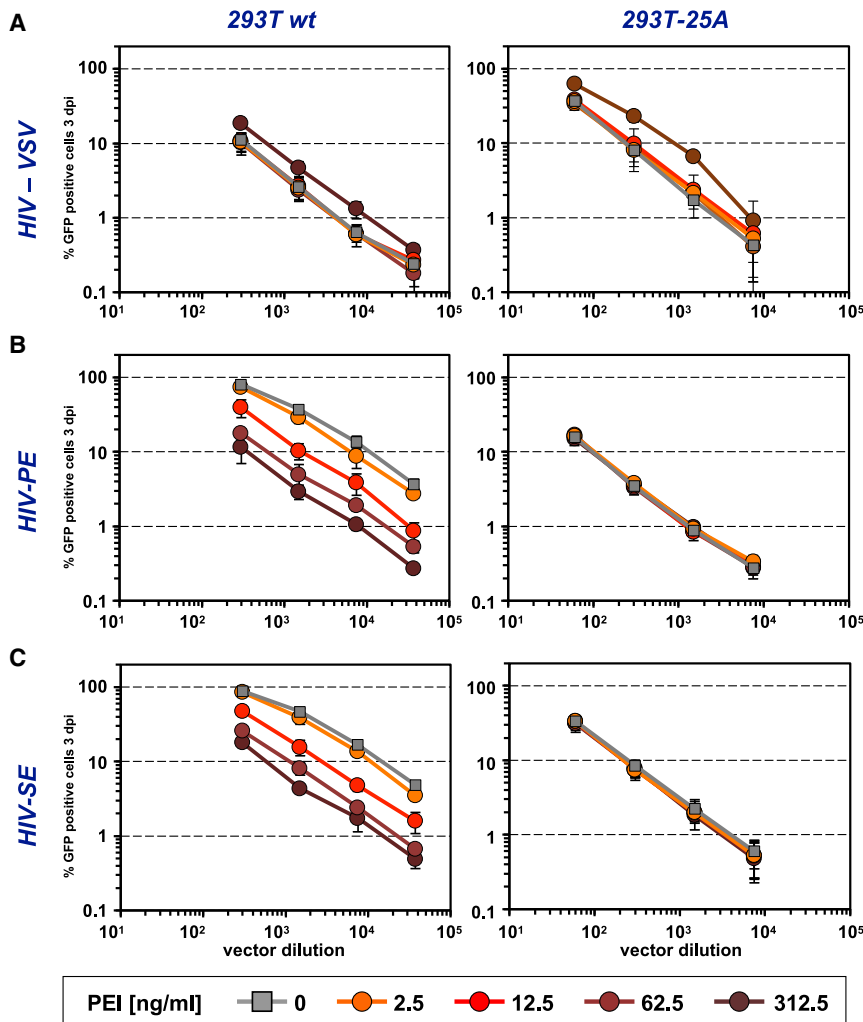


**Figure 7. Viral glycoprotein-dependent influence of exogenous PEI addition on retroviral vector transduction efficiency of different target cells**

WT 293T cells (293 WT) or PG-deficient (293T-25A) target cells were incubated with decreasing serial dilutions of GFP-expressing LV (HIV) vector particles pseudotyped with (A) VSV-G (VSV), (B) PFV (PE), or (C) SFVmac (SE) glycoproteins, derived by transient transfection of 293T-25A packaging cells using CaP transfection technique, that contained fixed concentrations of exogenously added PEI, as indicated. Three dpi, the percentage of GFP-expressing cells in the individual samples was determined by flow cytometry. Shown are the mean values  $\pm$  SD ( $n = 3$ ) of the percentage of GFP-expressing cells.

venting efficient Pol encapsidation. However, it is possible that there is an indirect influence of PEI on PFV PR function. A mechanism that can be envisioned is that PEI, in contrast to CaP, unnaturally accelerates the budding of PFV particles. This could result in Gag/Pol not being processed to its natural extent, as active PR cannot sufficiently interact with and cleave its substrates in the shortened time. Why does this phenomenon then only become apparent for PFV RCVs and not PFV SRVs? We speculate that in case of PEI-derived PFV SRVs, the inhibition of PFV Pol enzymatic functions is compensated by higher particle-associated Pol levels as consequence of Pol expression from packaging constructs *trans* compared with a more natural Pol expression *cis* in the proviral context, as it was demonstrated in previous studies.<sup>43,44</sup> If this is true, it would suggest that optimal titers of CaP-derived PFV SRVs can be achieved by using much lower amounts of Pol packaging constructs than is necessary when using PEI transfection.

increase in RCV titers relative to the respective virions produced by PEI transfection. The underlying cause of the increased Gag processing of CaP-derived virions is not fully clear. Perhaps the capsid encapsidation of FV Pol, which, unlike orthoretrovirus Pol, is translated as a separate protein and requires its precursor to interact with the viral genomic RNA (vgRNA) for encapsidation, is inhibited by intracellular PEI, which appears to be present for several days in PEI transfected cells,<sup>30</sup> resulting in suboptimal PR-RT levels in released virions. Alternatively, PFV PR activity, which is known to depend on PR-RT dimerization on the protease-activating RNA motif (PARM) secondary structure in PFV vgRNA, might be blocked by PEI present in packaging cells and/or copackaged into PFV capsids. The initial analysis of Pol encapsidation in PFV RCVs performed in this study (Figure 5A) seems to indicate that there is no dramatic decrease in overall particle-associated Pol levels, but Pol processing into mature p85<sup>PR-RT</sup> and p40<sup>IN</sup> subunits is also strongly inhibited in PEI-derived PFV RCVs. Thus, PEI appears to interfere with FV Pol enzymatic functions, most likely that of the PR, rather than pre-

using much lower amounts of Pol packaging constructs than is necessary when using PEI transfection.

Our results clearly demonstrate that free PEI or PEI/DNA complexes inhibit PFV GP-mediated infection of different target cell types in a dose- and HS-PG-dependent manner. Of the cell types examined, the ones most sensitive to inhibition were suspension cells of myeloid or lymphoid origin. Here, 2.5 ng/mL of exogenously added PEI already showed a clear inhibition. In contrast, inhibition on adherent cells required 10- to 100-fold higher PEI levels. This observation of the inhibitory effect of PEI is in good agreement with the HS staining data with anti-HS monoclonal antibody F58-10E4, where significantly higher HS concentrations were found for all parental adherent cells and very low or isotype-control-level concentrations for all suspension cells (Figure S3). This suggests that the amount of HS-PGs on the surface of a cell and the PEI concentrations required to bind them and exert an inhibitory effect on FV GP-mediated infection are directly correlated. Furthermore, the HS

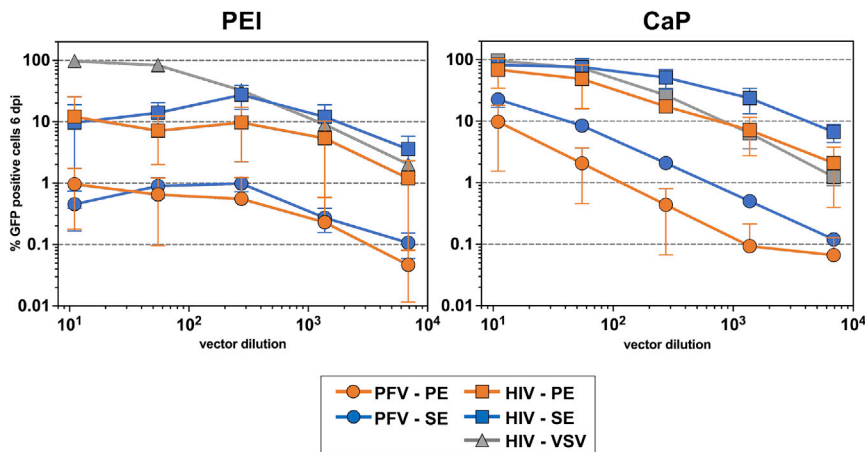


**Figure 8. Titration of PFV and HIV-1 retroviral vector supernatants harboring various viral glycoproteins and produced by calcium phosphate or polyethylene imine transfection using 293T-25A cells on THP-1 target cells**

Cell-free PFV (PFV) and LV (HIV) SRV supernatants harboring various viral GPs (VSV, PE, SE) were produced by transient transfection of PG-deficient 293T 25A packaging cells using the respective GFP encoding transfer vector plasmid and packaging construct combination by PEI or CaP transfection methodologies, as indicated. Subsequently, THP-1 target cells were incubated with decreasing serial dilutions of the respective vector supernatants as indicated. Six dpi, the percentage of GFP-expressing cells in the individual samples was determined by flow cytometry. Shown are the mean values  $\pm$  SD ( $n = 3$ ).

staining data using a different anti-HS monoclonal antibody (T320.11) suggests that the HS composition of THP-1 cells might be different from that of 293T, HT1080, and L929 cells. Thus, the specific HS composition may also influence its interactions with FV GP and PEI. Taken together, this may explain why inhibitory effects of PEI remnants, most likely being present in PEI-derived retroviral vector supernatants, may not have been noticed before in application of FV GP-containing vector supernatants on adherent target cell types. Conversely, this could also explain why suspension cells (of myeloid or lymphoid origin) and HS-deficient adherent Sog9 cells lack the positive effect of exogenously added PEI on infections with VSV-G pseudotypes. The known negative charge repulsion of sugar residues that can negatively influence viral transductions with VSV-G pseudotypes seems to play only a minor suppressive role in suspension cells with low HS-PG concentration and to have no effect on HS-deficient Sog9 cells. Interestingly, the novel HS-deficient 293T cell lines take on a rather unique role. On the one hand, the addition of PEI has no negative effect on transduction of 293T-25A with FV GP-containing vectors just as it does for Sog9 cells. In contrast to Sog9 cells, however, a positive effect could be observed on 293T-25A cells by adding PEI during transduction with VSV-G pseudotyped LV vectors. Presumably, the additional chondroitin sulphotransferase defect (C4ST1 in addition to Ext1) in Sog9 cells or their murine origin is the cause of this difference.<sup>45</sup>

The PG-deficient packaging cell lines generated in this study also represent a significant progress for potential application of FV vectors as gene transfer vehicles in preclinical and clinical settings. Since their use generally enable higher FV GP-containing vector titers on all target cells, less resources are required to produce similar amounts of infectious vector particles. Furthermore, the PG-deficient cells described in this study could also form the basis for novel stable retroviral producer cells. The significantly increased infectious titers of FV GP-containing retroviral vectors (and potentially those containing other heterologous GPs) obtained with PG-engineered producer cells could substantially reduce production costs with such cells. In this respect, our pioneering study clearly demonstrates the potential of ge-

netic engineering for improved retroviral vector production. In addition, probably similarly important will be the possibility to produce vector supernatants by transient transfection free of inhibiting polycation transfection reagent remnants, which according to our results are not easy to remove, at least by the methods examined in this study. Perhaps ion-exchange chromatography, frequently used as post-harvest purification method for retroviral vector clean up, might be able to remove PEI remnants. However, for establishing an effective post-harvest purification method, it would be critical to know whether the PEI-mediated target cell inhibition in FV vector supernatants is mediated by free PEI in solution or PEI in complex with PFV particles for example by PEI-GP interactions. In the latter case, ion-exchange chromatography might not work as well as in the former case. Inhibitor-free FV GP-containing vector preparations are essential for the correct determination of viral titers requiring a positive correlation of virus dose and transduction efficiency. Furthermore, they will be critical for efficient transduction of target cells with a low abundance of cell-surface HS-PG or specific HS-PG composition such as lymphoid and myeloid lineages and perhaps also for efficient gene transfer in *in vivo* settings as recently demonstrated in different animal models.<sup>46–49</sup>

In consideration of a potential use of these new PG-deficient packaging cell lines for large-scale vector production, several aspects need to be examined in the future.<sup>50</sup> Although large-scale, clinical-grade retroviral vector production can be accomplished using adherent culture of 293T packaging cells, for example, using cell factories, it often makes use of packaging cells adapted for growth in suspension and serum-free medium.<sup>51</sup> In the case of vector production by transient transfection, PEI is frequently used in this scenario. This most likely would result in similar inhibitory effects on FV GP-containing vector supernatants as described above for the production scenario involving adherent 293T cells. Therefore, the choice of transfection reagent used will be a critical factor. The transfection efficiency of CaP for suspension cells, as used in our study involving adherent packaging cell culture, might not be sufficient to achieve high-titered vector supernatants.<sup>52,53</sup> Therefore alternative chemical

or physical transfection methods like liposomes or electroporation should be examined. Due to these potential challenges, we would rather recommend the development of stable PG-deficient 293T packaging variants instead, which would also lower the contaminant load from residual plasmid for downstream purification processes. However, since it was observed previously that constitutive expression of PFV Gag appears to be toxic to 293T cells<sup>54</sup> (unpublished data), such an approach should involve an inducible expression of the FV packaging components, similar to how it has been established for LV vectors.<sup>55</sup>

A recent study involving the genomic, transcriptomic, and metabolic gene analysis of six of the most widely used HEK293 cell lines including adherent 293T and suspension 293F variants suggest no major differences in the expression of extracellular matrix organization gene sets between suspension and adherent 293 variants.<sup>56</sup> In contrast, suspension variants had significant upregulation of gene sets involved in cellular compartment organization such as cell morphogenesis and cell junction, cell membrane, and cytoskeleton organization. Therefore, a benefit of using the suspension-growth-adapted, PG-deficient 293T packaging cell lines compared with parental 293T cells for FV GP-containing vectors might be possible, although this has to be experimentally validated.

Finally, it will be interesting to explore in the future whether the use of the PG-deficient 293T packaging cells generated in this study will be beneficial for the production of retroviral vectors pseudotyped with other viral GPs, in particular those that are known to exploit PG interactions for initial attachment and/or target cell entry, such as GP variants of Ross River virus,<sup>57</sup> other alpha viruses,<sup>58</sup> or hepatitis C virus.<sup>59</sup> Similarly, the PG-deficient 293T cells should allow production of inhibitor-free MLV vectors using the amphotropic MLV GP, which were previously shown to be inhibited by secreted PG, in particular CS-PG, of NIH 3T3 packaging cells.<sup>60,61</sup> Not only retroviral vectors but also viral vectors based on other viruses or recombinant replication-competent variants of viruses such as AAV<sup>62</sup> or many herpes viruses<sup>63,64</sup> are known to naturally interact with PGs during entry and/or release. They are additional potential candidates whose virus production may be enhanced *in vitro* by using the PG-deficient 293T packaging cell line variants 293T-25A or 293T-306 instead of the commonly used parental cells.

## MATERIALS AND METHODS

### Cells and culture conditions

The human embryonic kidney cell line 293T (ATCC CRL-1573,<sup>65</sup>) as well as its HS-deficient variants 293T-25A and 293T-306 generated in this study and described below (see [B3GAT3 gene inactivation](#)); the human epithelial fibrosarcoma cell line HT1080 (ATCC CCL-121<sup>66</sup>) as well as the clonal variant HT1080 PLNE thereof containing a PFV LTR-driven EGFP reporter gene expression cassette;<sup>43</sup> and mouse fibroblast L cells (ATCC CRL-264,<sup>39</sup>) as well as its variant Sog9 with a defect in initiation of GAG assembly so that no surface HS is being produced (gift of F. Neipel, Erlangen<sup>39</sup>) were cultivated in Dulbecco's modified Eagle's medium (DMEM) supplemented

with 10% heat-inactivated fetal calf serum and antibiotics. The human T lymphocyte Jurkat cell line (ATCC TIB-152,<sup>67</sup>) and the human monocyte cell line THP-1 (ATCC TIB-202,<sup>68</sup>) were cultivated in RPMI supplemented with 10% heat-inactivated fetal calf serum, 1% non-essential amino acids, 1% sodium pyruvate, and 1% L-alanine, L-glutamate.

### Recombinant plasmid DNAs

Integration-competent, replication-deficient, single-round PFV (SFVpsc) vector supernatants were produced using a four-component system. It consists of the PFV transfer vector plasmid puc2MD9 (containing a spleen focus-forming virus U3 (SFFV U3) promoter-driven EGFP reporter gene expression cassette) and the expression-optimized packaging constructs pcoPG4 (PFV Gag), pcoPP (PFV Pol), pcoPE (PE), or pcoSE (SFVmac/SFVmyc Env), described previously.<sup>18,69</sup> The plasmids were cotransfected at a 13:3.3:1.5:1 ratio. In a few experiments, PFV SRVs were produced using a two-component PFV vector system consisting of the PFV Gag, Pol, and NLS-LacZ reporter gene cassette encoding transfer vector plasmids pczDWP02<sup>70,71</sup> or pMH120<sup>72</sup> and the PE encoding packaging construct pczHFVenv EM002<sup>8</sup> and were cotransfected at 1:1 ratio.

EGFP-expressing TraFo vector supernatants, enabling transient genetic modification of target cells by non-viral mRNA Transfer, were produced using a recently described three-component system, comprising pcoPG4 (PFV Gag), pcoPE (PE), or pcoSE (SFVmyc Env) packaging constructs and pcziEGFP transfer vector plasmid devoid of retroviral sequences<sup>49,73</sup> and were cotransfected at a 3.2:1:8.3 ratio. For production of TraFo particles pseudotyped with VSV-G, an expression-optimized version of a PFV Gag packaging plasmid (pcoPG4 M6<sup>74</sup>) encoding a PFV Gag protein with an N-terminal HIV-1 Gag matrix domain (MA) enabling PE-independent particle egress and pcziVSV-G were used in combination with the transfer vector plasmid<sup>25</sup> and cotransfected at a 1.1:1:2.9 ratio. The CMV-driven PFV proviral expression vector pczHSRV2 (WT), described previously,<sup>75</sup> was used for production of RCV supernatants.

Integration-competent, replication-deficient, single-round HIV vector supernatants were produced using the EGFP-expressing transfer vector plasmid p6NST60<sup>49</sup> (containing the identical SFFV U3-EGFP reporter gene cassette as the PFV puc2MD9 transfer vector plasmid, described above) in combination with the HIV-1 Gag-Pol expressing packaging vector pCD/NL-BH<sup>76</sup> and various Env packaging constructs described below. Integration-competent, replication-deficient, single-round MLV vector supernatants were produced using the transfer vector plasmid pczCFG2 fEGN<sup>4</sup> (containing a MLV LTR-driven EGFP-neomycin fusion protein expression cassette) in combination with the MLV Gag-Pol expressing packaging vector pHIT60<sup>77</sup> and various Env packaging constructs described below. For production of HIV and MLV pseudotyped with VSV-G- (pcziVSV-G<sup>25</sup>), PFV (SFVpsc) Env- (pcoPE01<sup>78</sup>) or SFVmac (SFVmyc) Env- (pcoSE03<sup>78</sup>) encoding packaging constructs were used. The following cotransfection ratios of transfer vector were



used: Gag/Pol: Env packaging plasmids were used: HIV-VSV or MLV-VSV, 3.5:3.5: 1; HIV-PE, HIV-SE, MLV-PE, or MLV-SE, 7:7:1.

### Viral vector production and harvest

Cell culture supernatants containing recombinant viral particles were generated by transfection of the corresponding plasmids into various packaging cells as indicated using either branched PEI, CaP coprecipitation, or PolyFect (Qiagen) techniques.

PEI transfection was essentially performed as described previously.<sup>43,49,69</sup> Briefly, retroviral vector system expression constructs were transfected into  $5 \times 10^6$  HEK293T cells seeded into 10 cm culture dishes 16 to 24 h earlier. The transfection mix was set up by mixing 15 to 16  $\mu\text{g}$  of total DNA, of the respective retroviral expression constructs at the appropriate ratios as described above (or pUC19 for mock supernatants), in 1 mL plain DMEM with 45–48  $\mu\text{g}$  PEI (Sigma-Aldrich Cat# 408727, 1 mg/mL in PBS) or in 1 mL plain DMEM and incubating for about 20 min. The transfection mix was carefully added to culture dishes containing the adherent cells in 4 mL DMEM (15% FCS). Transfected cells were incubated overnight at 37°C. After approximately 30 h, cells were deprived of old culture medium, washed with 6 mL PBS, and covered with 6 mL new culture medium DMEM (10% FCS) or plain DMEM for experiments involving further post-harvest purification procedures (see below). After a second night of incubation, virus particles were ready to be harvested (44–48 h after transfection).

For CaP transfection,  $5 \times 10^6$  packaging cells were seeded into 10 cm culture dishes 16–24 h in advance. Before transfection, the complete culture medium was exchanged by 8 mL DMEM (10% FCS) pre-equilibrated at 37°C, 5% CO<sub>2</sub> for at least 1 h. The transfection mix was set up by rapid addition of 1 mL 2 $\times$  HBS solution (50 mM HEPES [pH 7.05], 10 mM KCl, 12 mM Dextrose-H<sub>2</sub>O, 280 mM NaCl, 1.5 mM Na<sub>2</sub>HPO<sub>4</sub>) to 1 mL DNA solution (30  $\mu\text{g}$  of total DNA, 124  $\mu\text{L}$  2M CaCl<sub>2</sub>, and ddH<sub>2</sub>O in total volume of 1 mL) in 2 mL Eppendorf tubes and subsequent rapid mixing by vortexing for 10 s. After 30 s at room temperature, the transfection mix was added carefully but swiftly dropwise to the packaging cells in 10 cm dishes. After 6–8 h of incubation at 37°C, 5% CO<sub>2</sub>, the transfection mixture was aspirated and replaced by 8 mL fresh DMEM (10% FCS). In cases where sodium butyrate (NaBu) stimulation was employed, NaBu was added at 24 h post-transfection to 10 mM final concentration and incubation continued at 37°C, 5% CO<sub>2</sub>. At 30–32 h post-transfection, cells were deprived of old culture medium, washed with 6 mL PBS, and covered with 6 mL new culture medium DMEM (10% FCS) per 10 cm dish. After overnight incubation at 37°C, 5% CO<sub>2</sub>, at 44–48 h post-transfection, virus particles were ready to be harvested.

For PolyFect transfection,  $4.8 \times 10^6$  packaging cells were seeded into 10 cm culture dishes 16–24 h in advance. Before transfection, the complete culture medium was exchanged by 7.5 mL DMEM (10% FCS) pre-equilibrated at 37°C, 5% CO<sub>2</sub>, for at least 1 h. The transfection mix was set up by mixing in a 15 mL Falcon tube 285  $\mu\text{L}$  plain

DMEM, 16  $\mu\text{g}$  total DNA, and 75  $\mu\text{L}$  Polyfect, followed by vortexing for 10 s and incubation at room temperature for 10 min. Subsequently, 2.5 mL growth medium was added. Following mixing, the transfection mix was added carefully but swiftly dropwise to the packaging cells in 10 cm dishes.

To harvest cell-free virus supernatant, the medium in a culture dish was aspirated with a syringe and subsequently filtered through 0.45  $\mu\text{m}$  syringe sterile filter or transferred into Falcon tubes and cleared by low-speed centrifugation (600  $\times g$ , 5 min, room temperature). The virus-containing solution was snap frozen and stored at –80°C for later use.

Cell-bound virus supernatants were obtained by a single freeze-thaw cycle. After removal of the growth medium to harvest virus particles released into the supernatant (cell-free virus supernatant), as described above, 6 mL fresh culture medium DMEM (10% FCS) was added to the cell layer in the 10 cm dish. Subsequently, the dishes with medium were placed either on a metal plate sitting on dry ice for about 10 min or into a –80°C freezer for about 20 min, until fully frozen. Thereafter, the frozen dishes were placed into a tissue culture incubator (37°C, 5% CO<sub>2</sub>) until the liquid was fully thawed. Next the solution was gently but thoroughly mixed by pipetting up and down before transfer into Falcon tubes and centrifugation (5 min, 1,000  $\times g$ , 4°C) to pellet cellular debris. Finally, the supernatant, except for a small volume above the debris pellet, was transferred to a fresh tube, aliquoted, and stored as described above.

### Post-harvest vector supernatant purification

Three different purification protocols were explored for potential removal of PEI remnants in harvested, cell-free plain retroviral vector supernatants (Figure 4A). For all approaches, retroviral vector supernatants lacking FCS and produced by transient transfection using PEI were used. First, for UC, 30 mL plain, cell-free vector supernatants were pelleted by centrifugation in SW-32Ti rotors at 25,000 RPM (~82,600  $g_{\text{ave}}$ ) at 4°C for 90 min. After discarding the supernatant, the virus pellet was gently resuspended in 17.5 mL growth medium (DMEM, 10% FCS) and 500  $\mu\text{L}$  aliquots snap frozen, followed by storage at –80°C. Second, for UC and UF, 30 mL plain, cell-free vector supernatants were pelleted by UC as described above but gently resuspended in 500  $\mu\text{L}$  PBS. Subsequently, the concentrated vector supernatants were transferred to Amicon Ultra-0.5 100K Centrifugal Filter Devices, pre-equilibrated with DNase-RNase-free ddH<sub>2</sub>O, and centrifuged at 14,000  $\times g$  for 5 min. The flow through was discarded, and after adding 450  $\mu\text{L}$  sterile PBS, the filter device was centrifuged again at 14,000  $\times g$  for 10 min. After discarding the flow through, the filter device was inverted, placed into a collection tube, and centrifuged at 1,000  $\times g$  for 2 min to harvest the purified and concentrated vector supernatant (~40  $\mu\text{L}$ ). After gentle resuspension in 500  $\mu\text{L}$  growth medium the concentrated virus supernatant was transferred to a 50 mL Falcon tube and mixed with 17 mL growth medium. Finally 500  $\mu\text{L}$  aliquots were snap frozen and stored at –80°C. Third, for SEC, CaptoCore 700 resin (Cytiva), 2.5 mL slurry, was transferred into centrifuge columns (Pierce, Cat# 89898), placed in 50 mL Falcon tubes, and equilibrated with 30 mL sterile PBS by gravity flow draining. In the

meantime, 20 mL cell-free vector supernatants in a Falcon tube were supplemented with Benzonase to 100 U/mL and incubated in a water-bath at 37°C for 30 min. Subsequently, the vector supernatant was added to the top of the CaptoCore gel bed, and the column was drained until all liquid had entered. The flow through was harvested and 500  $\mu$ L aliquots were snap frozen, followed by storage at  $-80^{\circ}\text{C}$ .

### Target cell infection

Frozen aliquots of plain, cell-free vector supernatants were used without addition of any additives (e.g., polybrene, protamine sulfate, PEI), if not stated otherwise, for the transduction of target cells. Adherent cells were seeded at a density of  $2.5 \times 10^4$  per well (in a 12-well plate, 1 mL growth medium per well) and incubated overnight at 37°C. The following day, the culture medium was aspirated and replaced with virus-containing solution in an end volume of 1 mL. Virus supernatants were used undiluted or diluted as indicated. If different virus solutions were combined, the ratio was 1:1 if not stated otherwise. After approximately 5 h of incubation, the virus supernatant was replaced by the same volume of fresh growth medium. Usually, cells were used for further experiments (generally fluorescence-activated cell sorting [FACS] analysis, see below) at 72 h post-infection. Viral titers were then calculated from the percentage of fluorescent-reporter-positive cells as described previously and are given as EGFP transducing units (EGFP TU/mL).<sup>25</sup>

For transductions of suspension cells per well,  $1 \times 10^5$  cells in 50  $\mu$ L volume were added to 500  $\mu$ L undiluted or diluted virus supernatant in 24-well plates. When undiluted supernatants were employed, virus supernatant incubation was terminated 4–6 h later by transfer of individual samples into 1.5 mL Eppendorf tubes, pelleting the cells by centrifugation ( $600 \times g$ , 5 min, room temperature), discarding the supernatant, gentle resuspension of the cell pellet in 500  $\mu$ L fresh growth medium, and transfer into a fresh 24-well plate, followed by incubation at 37°C, 5%  $\text{CO}_2$ , until further analysis as indicated. When only virus dilutions ( $10^{-1}$  or lower) were employed, virus supernatants were left on the cells until further analysis at later time points, generally at 48–72 h post-infection.

### Physical vector titers

Physical titers of HIV and MLV vector supernatants were determined by a qPCR-based product-enhanced RT (PERT) assay similarly as described previously.<sup>79,80</sup> Briefly, 5  $\mu$ L of 1:100 diluted plain vector supernatant were mixed with 5  $\mu$ L  $2\times$  lysis buffer (100 mM Tris [pH 7.4], 50 mM KCl, 0.25% [v/v] Triton X-100, 40% [v/v] Glycerol; 400 U/mL RiboLock RNase inhibitor added prior to use) and incubated for 20 min at room temperature. Subsequently, the sample was diluted 1:5 by addition of 40  $\mu$ L ddH<sub>2</sub>O. For qPCR amplification, 5  $\mu$ L of diluted sample or standard was mixed in duplicates with 20  $\mu$ L PERT qPCR mix composed of 2.79 nM mM MS2 RNA (Roche), 0.5  $\mu$ M fwd (5'-TGCTCGCGGATACCCG-3') and rev (5'-AACTT GCGTTCTCGAGCGAT-3') MS2 primer, 0.25  $\mu$ M MS2 probe (5'-HEX-ACCTCGGGTTTCCGTCTTGCTCGT-BHQ2 3'), 0.5  $\mu$ M ROX reference dye, and 1.25 $\times$  Maxima Probe Master Mix (Thermo Scientific). Amplifications were performed on a OneStepPlus

(Applied Biosystems) with one cycle at 42°C for 20 min, 95°C for 2 min for reverse transcription, followed by 40 cycles of 95°C for 30 s, 58°C for 30 s, and 72°C for 30 s for amplification. As standard 5  $\mu$ L of a 10-fold dilution series of recombinant HIV-1 RT (Abcam #ab63979; 2 mU/ $\mu$ L in DMEM, 10% FCS) was used in the range of  $10^5$ – $10^0$  nU RT/reaction. Infectious and physical titers of vector supernatants employed in this study are summarized in Table S1.

### Western blot analysis

For western blot analysis of viral particle protein composition, about 10 mL cell-free virus supernatant was carefully layered onto 2 mL 20% sucrose in ultracentrifuge tubes. Virus particles were pelleted by centrifugation in SW-32Ti rotors at 25,000 RPM ( $\sim 82,600 g_{\text{ave}}$ ) at 4°C for 90 min. After discarding the supernatant, the virus pellet was resuspended in  $1\times$  protein sample buffer (40 mM Tris [pH 7.6]; 8% (v/v) glycerol; 3% (w/v) SDS; 0.1 M DTT; 0.01% (w/v) Coomassie Blue G 250), boiled for 5 min at 95°C, and stored at  $-20^{\circ}\text{C}$  until further use.

Protein lysates of packaging cells were obtained by washing the cell layer once with PBS after removal of the growth medium containing the released virus particles. After aspiration of the PBS, 600  $\mu$ L cold  $1\times$  lysis buffer (10 mM Tris [pH 8.0]; 140 mM NaCl; 0.025 NaN<sub>3</sub>; 1% (v/v) Triton X-100) per 10 cm dish was added to the cell layer and incubated on a rocking platform for 20 min at 4°C. Subsequently, cells were scraped of the dish using a rubber policeman, and the whole suspension was transferred to QIAshredder in a 2 mL Eppendorf tube. After centrifugation at 13,000 RPM for 2 min at 4°C in a table top centrifuge, 600  $\mu$ L  $2\times$  protein sample buffer was added to the QIAshredder, followed by another 2 min centrifugation step. Both eluates were combined, gently mixed, boiled at 95°C for 10 min, and stored at  $-20^{\circ}\text{C}$  until further use.

Aliquots of virus and/or cell protein lysates were loaded onto commercial precast or selfmade 7.5% Tricine PAGE. After separation in an electric field, the proteins were transferred to nitrocellulose membranes by semidry blotting. After blocking of nitrocellulose membranes in PBS-T (PBS, 0.5% Tween 20) with 5% skim milk for 2 h, membranes were washed twice briefly with PBS-T. Subsequently, membranes were incubated with primary antibody solution in PBS-T with 5% skim milk for 1 h to overnight at room temperature or 4°C, followed by two brief and three 5 min washes in PBS-T. Next, second appropriate horseradish peroxidase (HRP) coupled second step reagents in PBS-T with 5% skim milk were added and incubated for 1 h at room temperature. After two brief and three 10 min washes in PBS-T and careful removal of all excess liquid, the membrane was incubated with chemoluminescent HRP substrate for 1 min. Finally, after removal of excess substrate, chemoluminescent signals of membranes wrapped in Saran wrap were digitally recorded using a Fuji LAS-3000 bioimager and LAS software v.2.2.

### Flow cytometry analysis

For analysis of GFP expression, transduced adherent target cells were trypsinized and transferred to FACS tubes containing 2 mL of cold

PBS, whereas suspension cells were directly transferred. Following centrifugation (1,200 RPM, 5 min, 4°C), pelleted cells were resuspended in 300 µL FACS buffer (PBS with 2% [v/v] FCS and 0.1% [w/v] sodium azide) and stored on ice until analyzed by flow cytometry.

For analysis of cell surface HS expression, cells were first detached from culture surfaces (in case of adherent cultures) using only PBS-EDTA solution without trypsin, since the latter is known to destroy PG molecules on cell surfaces. Both cell types ( $1 \times 10^5$ ) derived from either adherent or suspension cultures were then transferred to FACS tubes containing 2 mL FACS buffer and centrifuged (1,200 RPM, 5 min, 4°C). After discarding the supernatant, cell pellets were resuspended in 100 µL primary antibody solution, containing 0.1–0.5 µg antibody diluted in 100 µL FACS buffer, and incubated on ice for 30 min. After the first incubation, a washing step was executed by suspending cells in 4 mL FACS buffer and centrifuging them again (1,200 RPM, 5 min, 4°C). The supernatant was discarded, and cell pellets were resuspended in 100 µL secondary antibody solution, containing 0.1–0.175 µg fluorophore-coupled anti-primary antibody diluted in 100 µL FACS buffer. The secondary antibody was incubated for 30 min on ice and in the dark to minimize the bleaching effect on the fluorochromes. As a last step, cells were washed again and resuspended in 300 µL FACS buffer for analysis by flow cytometry on a FACS Calibur (Becton-Dickinson, Heidelberg, Germany) or MACSQuant VYB (Miltenyi, Bergisch Gladbach, Germany) instrument. For cell sorting, a FACS Aria II (Becton-Dickinson, Heidelberg, Germany) was used. Results from FACS measurements were analyzed using the software programs CellQuest Pro and FlowJo (both Becton-Dickinson, Heidelberg, Germany).

### Antibodies

For flow cytometry analysis, mouse anti-HS (F58-10E4, immunoglobulin M [IgM], amsbio, Cat# 370255), mouse anti-heparin/HS (T320.11, IgG1, Millipore, Cat# MAB2040), mouse IgM K isotype control (Pharmingen, Cat# 557275), mouse IgG2a K isotype control (Pharmingen, Cat# 03021D), Alexa 488-conjugated goat anti-mouse IgM+IgG (H + L) (Jackson ImmunoResearch, Cat# 115-545-068), and PE-conjugated goat anti-mouse IgM+IgG (H + L) (Jackson ImmunoResearch, Cat# 115-116-068) were used. For western blot analysis, polyclonal rabbit anti-sera specific for PFV Gag,<sup>4</sup> the PE LP,<sup>81</sup> or monoclonal antibodies specific for PFV Pol PR-RT or PFV Pol IN<sup>82</sup> and HRP-coupled polyclonal goat anti-mouse Igs (Dako P0447) or swine anti-rabbit Igs (Dako P0217) were used.

### B3GAT3 gene inactivation

293T packaging cell variants with inactivated *B3GAT3* ORF were generated using a recently published PFV-based, two-component CRISPR-Cas9 vector system (TraFo) consisting of Cas9-encoding TraFo vectors, which are combined with single guide RNA (sgRNA)-encoding, integration-competent (ICPV) PFV retroviral vectors.<sup>73</sup> The seed sequences of the sgRNAs specific for the human *B3GAT3* ORF selected by CRISPRscan<sup>83</sup> and employed for this study are listed in Table S2. Briefly, parental, WT HEK293T cells were transduced with

various combinations of TraFo-Cas9 and ICPV-*B3GAT3*sgRNA supernatants, harboring an additional dsRed Ex2 reporter protein expression cassette, or respective controls. Two and 9 days post-transduction (p.t.), cell-surface HS expression of the individual cell populations was examined by immunostaining and flow cytometry. The three cell populations (#5: p660 sgRNA; #6: p56 + p608 sgRNAs; #8: p72 + p608 sgRNAs) with the strongest reduction in cell-surface HS expression were used at day 14 p.t. to set up for subcloning of cell clones by limiting dilutions in 96-well plates. Furthermore, population #6 was chosen on day 21 p.t. for immunostaining with anti-HS antibodies under sterile conditions, and HS-negative cells were single-cell sorted into 96-well plates using a FACS Aria II (Becton-Dickinson) device. Individual clones of both approaches were expanded and screened by flow cytometric analysis of HS cell-surface expression. HS cell-surface-negative clones (23 of 330 total) were further expanded. HS cell-surface expression of individual clones was reanalyzed at least once, and stock aliquots were generated. HS-negative single-cell clones were only obtained from population #6, with one clone from the limiting dilution and 22 clones from the single-cell sorting approach. Two clones designated as 293T-25A (clone 10-4E2) and 293T-306 (clone 10-1F10) did not express dsRed Ex2, indicating that they lack a stably integrated *B3GAT3* sgRNA expression cassette. These clones were chosen for further characterization with respect to their properties as viral packaging cell lines. Genetic characterization of the clones involved amplification of genomic fragments (Figure S9) harboring the p56 (1310 bp) and p608 sgRNA target locus (560 bp) using primer sets listed in Table S4. Sanger sequencing revealed insertion or deletion (indel) mutations at the p56 and WT sequences at the p608 sgRNA target locus in 293T-25A and 293T-306 cells (Figure S9B). The indel sequences at the p56 locus were determined by next-generation sequencing (NGS) analysis using amplification primers with the NGS adaptors listed in Table S4. Raw amplicon sequence reads were processed using R v.4.0.2 software package dada2 (v.1.16.0).<sup>84</sup> Raw sequences were first filtered and trimmed with the following parameters: maximum ambiguity: 0; number of expected errors for each read: 1; truncate reads at the first instance of a quality score less than 2. After quality filtering, reads were merged as contigs, and detected chimera were removed with default parameters. Then, amplicon sequence variants were called, and the counts of each amplicon sequence variant in each sample were calculated. The analysis revealed that both cell lines harbor three different mutant *B3GAT3* alleles, all resulting in frame shifts and severely truncated *B3GAT3* proteins (Figure S9C). As both the 293T-25A and 293T-306 cell lines harbor the same *B3GAT3* alleles and are derived from the same knockout (KO) target cell population, it cannot be excluded that the same KO clone was isolated twice by the independent selection schemes.

### Statistics

All the statistical analyses were performed using GraphPad Prism 9. The numbers of experimental replicates and information on the statistical methods used for determination of two-tailed p values are described in the individual figure legends. Symbols represent: \*p < 0.05; \*\*p < 0.01; \*\*\*p < 0.001; \*\*\*\*p < 0.0001; ns: not significant (p ≥ 0.05).

## DATA AVAILABILITY

All authors declare that data are available within the article or the [supplemental information](#). Sequencing raw data (fastq files) are available upon request.

## SUPPLEMENTAL INFORMATION

Supplemental information can be found online at <https://doi.org/10.1016/j.omtm.2022.07.004>.

## ACKNOWLEDGMENTS

This work was supported by a grant from the Deutsche Forschungsgemeinschaft (DFG: SPP1923 LI 621/11-1) to D.L., and R.B. was funded by the German Research Foundation – project ID 369799452 – TRR237/B19. We acknowledge support by the Open Access Publication Funds of the SLUB/TU Dresden.

## AUTHOR CONTRIBUTIONS

Conceptualization, D.L.; methodology, C.M.M., H.K., F.L., and D.L.; verification, C.M.M., H.K., and D.L.; formal analysis, D.L.; investigation, C.M.M., H.K., A.E., S.R., D.W., N.S., B.Y., and R.B.; writing – original draft preparation, F.L. and D.L.; writing – review & editing, C.M., S.R., D.W., F.L., and D.L.; visualization, D.L.; supervision, D.L.; project administration, D.L.; funding acquisition, D.L.

## DECLARATION OF INTERESTS

D.L., S.R., and F.L. are inventors on patents filed by the Technische Universität Dresden on FV vector technologies.

## REFERENCES

- Rethwilm, A., and Lindemann, D. (2013). Foamy viruses. In *Fields Virology*, Sixth edition, 2, D.M. Knipe and P.M. Howley, eds (Lippincott Williams & Wilkins, a Wolters Kluwer Business), pp. 1613–1632.
- Khan, A.S., Bodem, J., Buseyne, F., Gessain, A., Johnson, W., Kuhn, J.H., Kuzmak, J., Lindemann, D., Linial, M.L., Löchelt, M., et al. (2018). Spumaretroviruses: updated taxonomy and nomenclature. *Virology* 516, 158–164.
- Lindemann, D., Hütter, S., Wei, G., and Löchelt, M. (2021). The unique, the known, and the unknown of spumaretrovirus assembly. *Viruses* 13.
- Lindemann, D., Pietschmann, T., Picard-Maureau, M., Berg, A., Heinkelein, M., Thurow, J., Knaus, P., Zentgraf, H., and Rethwilm, A. (2001). A particle-associated glycoprotein signal peptide essential for virus maturation and infectivity. *J. Virol.* 75, 5762–5771.
- Wilk, T., Geiselhart, V., Frech, M., Fuller, S.D., Flügel, R.M., and Löchelt, M. (2001). Specific interaction of a novel foamy virus Env leader protein with the N-terminal Gag domain. *J. Virol.* 75, 7995–8007.
- Fischer, N., Heinkelein, M., Lindemann, D., Ennsle, J., Baum, C., Werder, E., Zentgraf, H., Müller, J.G., and Rethwilm, A. (1998). Foamy virus particle formation. *J. Virol.* 72, 1610–1615.
- Baldwin, D.N., and Linial, M.L. (1998). The roles of Pol and Env in the assembly pathway of human foamy virus. *J. Virol.* 72, 3658–3665.
- Pietschmann, T., Heinkelein, M., Heldmann, M., Zentgraf, H., Rethwilm, A., and Lindemann, D. (1999). Foamy virus capsids require the cognate envelope protein for particle export. *J. Virol.* 73, 2613–2621.
- Geiselhart, V., Schwantes, A., Bastone, P., Frech, M., and Löchelt, M. (2003). Features of the Env leader protein and the N-terminal Gag domain of feline foamy virus important for virus morphogenesis. *Virology* 310, 235–244.
- Goldstone, D.C., Flower, T.G., Ball, N.J., Sanz-Ramos, M., Yap, M.W., Ogrodowicz, R.W., Stanke, N., Reh, J., Lindemann, D., Stoye, J.P., and Taylor, I.A. (2013). A unique spumavirus gag N-terminal domain with functional properties of orthoretroviral matrix and capsid. *PLoS Pathog.* 9, e1003376.
- Alke, A., Schwantes, A., Kido, K., Flötenmeyer, M., Flügel, R.M., and Löchelt, M. (2001). The bet gene of feline foamy virus is required for virus replication. *Virology* 287, 310–320.
- Yu, S.F., Eastman, S.W., and Linial, M.L. (2006). Foamy virus capsid assembly occurs at a pericentriolar region through a cytoplasmic targeting/retention signal in *Gag*. *Traffic* 7, 966–977.
- Liu, Y., Betts, M.J., Lei, J., Wei, G., Bao, Q., Kehl, T., Russell, R.B., and Löchelt, M. (2016). Mutagenesis of N-terminal residues of feline foamy virus Gag reveals entirely distinct functions during capsid formation, particle assembly, Gag processing and budding. *Retrovirology* 13, 57.
- Kong, X.H., Yu, H., Xuan, C.H., Wang, J.Z., Chen, Q.M., and Geng, Y.Q. (2005). The requirements and mechanism for capsid assembly and budding of bovine foamy virus. *Arch. Virol.* 150, 1677–1684.
- Lecellier, C.H., Neves, M., Giron, M.L., Tobaly-Tapiero, J., and Saïb, A. (2002). Further characterization of equine foamy virus reveals unusual features among the foamy viruses. *J. Virol.* 76, 7220–7227.
- Hill, C.L., Bieniasz, P.D., and McClure, M.O. (1999). Properties of human foamy virus relevant to its development as a vector for gene therapy. *J. Gen. Virol.* 80, 2003–2009.
- Mergia, A., Leung, N.J., and Blackwell, J. (1996). Cell tropism of the simian foamy virus type 1 (SFV-1). *J. Med. Primatol.* 25, 2–7.
- Stirnagel, K., Lüftenegger, D., Stange, A., Swiersy, A., Müllers, E., Reh, J., Stanke, N., Grosse, A., Chiantia, S., Keller, H., et al. (2010). Analysis of prototype foamy virus particle-host cell interaction with autofluorescent retroviral particles. *Retrovirology* 7, 45.
- Plochmann, K., Horn, A., Gschmack, E., Armbruster, N., Krieg, J., Wiktorowicz, T., Weber, C., Stirnagel, K., Lindemann, D., Rethwilm, A., and Scheller, C. (2012). Heparan sulfate is an attachment factor for foamy virus entry. *J. Virol.* 86, 10028–10035.
- Nasimuzzaman, M., and Persons, D.A. (2012). Cell Membrane-associated heparan sulfate is a receptor for prototype foamy virus in human, monkey, and rodent cells. *Mol. Ther.* 20, 1158–1166.
- Lindemann, D., Bock, M., Schweizer, M., and Rethwilm, A. (1997). Efficient pseudotyping of murine leukemia virus particles with chimeric human foamy virus envelope proteins. *J. Virol.* 71, 4815–4820.
- Russell, D.W., and Miller, A.D. (1996). Foamy virus vectors. *J. Virol.* 70, 217–222.
- Leurs, C., Jansen, M., Pollok, K.E., Heinkelein, M., Schmidt, M., Wissler, M., Lindemann, D., Von Kalle, C., Rethwilm, A., Williams, D.A., and Hanenberg, H. (2003). Comparison of three retroviral vector systems for transduction of nonobese diabetic/severe combined immunodeficiency mice repopulating human CD34+ cord blood cells. *Hum. Gene Ther.* 14, 509–519.
- Wurm, M., Schambach, A., Lindemann, D., Hanenberg, H., Ständker, L., Forssmann, W.G., Blasczyk, R., and Horn, P.A. (2010). The influence of semen-derived enhancer of virus infection on the efficiency of retroviral gene transfer. *J. Gene Med.* 12, 137–146.
- Ho, Y.P., Schnabel, V., Swiersy, A., Stirnagel, K., and Lindemann, D. (2012). A small-molecule-controlled system for efficient pseudotyping of prototype foamy virus vectors. *Mol. Ther.* 20, 1167–1176.
- Couteaudier, M., Calzada-Fraile, D., Montange, T., Gessain, A., and Buseyne, F. (2020). Inhibitors of the interferon response increase the replication of gorilla simian foamy viruses. *Virology* 541, 25–31.
- Sarrazin, S., Lamanna, W.C., and Esko, J.D. (2011). Heparan sulfate proteoglycans. *Cold Spring Harb. Perspect. Biol.* 3, a004952.
- Ströh, L.J., and Stehle, T. (2014). Glycan engagement by viruses: receptor switches and specificity. *Annu. Rev. Virol.* 1, 285–306.
- Iozzo, R.V., and Schaefer, L. (2015). Proteoglycan form and function: a comprehensive nomenclature of proteoglycans. *Matrix Biol.* 42, 11–55.
- Nomani, A., Hyvönen, Z., Pulkkinen, E., Hiekkala, M., and Ruponen, M. (2014). Intracellular gene delivery is dependent on the type of non-viral carrier and defined by the cell surface glycosaminoglycans. *J. Control. Release* 187, 59–65.



31. Paris, S., Burlacu, A., and Durocher, Y. (2008). Opposing roles of syndecan-1 and syndecan-2 in polyethyleneimine-mediated gene delivery. *J. Biol. Chem.* *283*, 7697–7704.
32. Payne, C.K., Jones, S.A., Chen, C., and Zhuang, X. (2007). Internalization and trafficking of cell surface proteoglycans and proteoglycan-binding ligands. *Traffic* *8*, 389–401.
33. Hadigal, S.R., Agelidis, A.M., Karasneh, G.A., Antoine, T.E., Yakoub, A.M., Ramani, V.C., Djalilian, A.R., Sanderson, R.D., and Shukla, D. (2015). Heparanase is a host enzyme required for herpes simplex virus-1 release from cells. *Nat. Commun.* *6*, 6985.
34. Agelidis, A., and Shukla, D. (2020). Heparanase, heparan sulfate and viral infection. *Adv. Exp. Med. Biol.* *1221*, 759–770.
35. Leurs, C. (2003). Etablierung foamyviraler Vektoren zur Transduktion humaner hämatopoetischer Stammzellen. In *Mathematisch-Naturwissenschaftliche Fakultät (Universität Düsseldorf)*, p. 101.
36. Westphal, D. (2003). Analyse der Interaktion heterologer Foamyvirus Hüllproteine und Kapside. In *Mathematisch-Naturwissenschaftliche Fakultät (Technische Universität Dresden)*, p. 88. Diploma.
37. Loh, P.C., and Ang, K.S. (1981). Replication of human syncytium-forming virus in human cells: effect of certain biological factors and selective chemicals. *J. Med. Virol.* *7*, 67–73.
38. Yu, S.F., Stone, J., and Linial, M.L. (1996). Productive persistent infection of hematopoietic cells by human foamy virus. *J. Virol.* *70*, 1250–1254.
39. Banfield, B.W., Leduc, Y., Esford, L., Schubert, K., and Tufaro, F. (1995). Sequential isolation of proteoglycan synthesis mutants by using herpes simplex virus as a selective agent: evidence for a proteoglycan-independent virus entry pathway. *J. Virol.* *69*, 3290–3298.
40. Mizumoto, S., Yamada, S., and Sugahara, K. (2014). Human genetic disorders and knockout mice deficient in glycosaminoglycan. *BioMed Res. Int.* *2014*, 495764.
41. Ennsle, J., Fischer, N., Moebes, A., Mauer, B., Smola, U., and Rethwilm, A. (1997). Carboxy-terminal cleavage of the human foamy virus Gag precursor molecule is an essential step in the viral life cycle. *J. Virol.* *71*, 7312–7317.
42. Zemba, M., Wilk, T., Rutten, T., Wagner, A., Flügel, R.M., and Löchelt, M. (1998). The carboxy-terminal p3Gag domain of the human foamy virus Gag precursor is required for efficient virus infectivity. *Virology* *247*, 7–13.
43. Hütter, S., Müllers, E., Stanke, N., Reh, J., and Lindemann, D. (2013). Prototype foamy virus protease activity is essential for intraparticle reverse transcription initiation but not absolutely required for uncoating upon host cell entry. *J. Virol.* *87*, 3163–3176.
44. Swiersy, A., Wiek, C., Reh, J., Zentgraf, H., and Lindemann, D. (2011). Orthoretroviral-like prototype foamy virus Gag-Pol expression is compatible with viral replication. *Retrovirology* *8*, 66.
45. Uyama, T., Ishida, M., Izumikawa, T., Trybala, E., Tufaro, F., Bergström, T., Sugahara, K., and Kitagawa, H. (2006). Chondroitin 4-O-sulfotransferase-1 regulates E disaccharide expression of chondroitin sulfate required for herpes simplex virus infectivity. *J. Biol. Chem.* *281*, 38668–38674.
46. Burtner, C.R., Beard, B.C., Kennedy, D.R., Wohlfahrt, M.E., Adair, J.E., Trobridge, G.D., Scharenberg, A.M., Torgerson, T.R., Rawlings, D.J., Felsburg, P.J., and Kiem, H.P. (2014). Intravenous injection of a foamy virus vector to correct canine SCID-X1. *Blood* *123*, 3578–3584.
47. Counsell, J.R., Karda, R., Diaz, J.A., Carey, L., Wiktorowicz, T., Buckley, S.M.K., Ameri, S., Ng, J., Baruteau, J., Almeida, F., et al. (2018). Foamy virus vectors transduce visceral organs and hippocampal structures following in vivo delivery to neonatal mice. *Mol. Ther. Nucleic Acids* *12*, 626–634.
48. Khattak, S., Sandoval-Guzmán, T., Stanke, N., Protze, S., Tanaka, E.M., and Lindemann, D. (2013). Foamy virus for efficient gene transfer in regeneration studies. *BMC Dev. Biol.* *13*, 17.
49. Hamann, M.V., Stanke, N., Müllers, E., Stirnagel, K., Hütter, S., Artegiani, B., Bragado Alonso, S., Calegari, F., and Lindemann, D. (2014). Efficient transient genetic manipulation in vitro and in vivo by prototype foamy virus-mediated nonviral RNA transfer. *Mol. Ther.* *22*, 1460–1471.
50. Perry, C., and Rayat, A. (2021). Lentiviral vector bioprocessing. *Viruses* *13*.
51. Bauler, M., Roberts, J.K., Wu, C.C., Fan, B., Ferrara, F., Yip, B.H., Diao, S., Kim, Y.L., Moore, J., Zhou, S., et al. (2020). Production of lentiviral vectors using suspension cells grown in serum-free media. *Mol. Ther. Methods Clin. Dev.* *17*, 58–68.
52. Gutiérrez-Granados, S., Cervera, L., Kamen, A.A., and Gòdia, F. (2018). Advancements in mammalian cell transient gene expression (TGE) technology for accelerated production of biologics. *Crit. Rev. Biotechnol.* *38*, 918–940.
53. Feng, L., Guo, M., Zhang, S., Chu, J., Zhuang, Y., and Zhang, S. (2007). Optimization of transfection mediated by calcium phosphate for plasmid rAAV-LacZ (recombinant adeno-associated virus-beta-galactosidase reporter gene) production in suspension-cultured HEK-293 (human embryonic kidney 293) cells. *Biotechnol. Appl. Biochem.* *46*, 127–135.
54. Wu, M., and Mergia, A. (1999). Packaging cell lines for simian foamy virus type 1 vectors. *J. Virol.* *73*, 4498–4501.
55. Chen, Y.H., Pallant, C., Sampson, C.J., Boiti, A., Johnson, S., Brazauskas, P., Hardwicke, P., Marongiu, M., Marinova, V.M., Carmo, M., et al. (2020). Rapid lentiviral vector producer cell line generation using a single DNA construct. *Mol. Ther. Methods Clin. Dev.* *19*, 47–57.
56. Malm, M., Saghaleyni, R., Lundqvist, M., Giudici, M., Chotteau, V., Field, R., Varley, P.G., Hattton, D., Grassi, L., Svensson, T., et al. (2020). Evolution from adherent to suspension: systems biology of HEK293 cell line development. *Sci. Rep.* *10*, 18996.
57. Kesari, A.S., Sharkey, C.M., and Sanders, D.A. (2019). Role of heparan sulfate in entry and exit of Ross River virus glycoprotein-pseudotyped retroviral vectors. *Virology* *529*, 177–185.
58. Gardner, C.L., Ebel, G.D., Ryman, K.D., and Klimstra, W.B. (2011). Heparan sulfate binding by natural eastern equine encephalitis viruses promotes neurovirulence. *Proc. Natl. Acad. Sci. USA* *108*, 16026–16031.
59. Barth, H., Schafer, C., Adah, M.I., Zhang, F., Linhardt, R.J., Toyoda, H., Kinoshita-Toyoda, A., Toida, T., Van Kuppevelt, T.H., Depla, E., et al. (2003). Cellular binding of hepatitis C virus envelope glycoprotein E2 requires cell surface heparan sulfate. *J. Biol. Chem.* *278*, 41003–41012.
60. Le Doux, J.M., Morgan, J.R., and Yarmush, M.L. (1999). Differential inhibition of retrovirus transduction by proteoglycans and free glycosaminoglycans. *Biotechnol. Prog.* *15*, 397–406.
61. Le Doux, J.M., Morgan, J.R., Snow, R.G., and Yarmush, M.L. (1996). Proteoglycans secreted by packaging cell lines inhibit retrovirus infection. *J. Virol.* *70*, 6468–6473.
62. Summerford, C., and Samulski, R.J. (1998). Membrane-associated heparan sulfate proteoglycan is a receptor for adeno-associated virus type 2 virions. *J. Virol.* *72*, 1438–1445.
63. Shieh, M.T., WuDunn, D., Montgomery, R.I., Esko, J.D., and Spear, P.G. (1992). Cell surface receptors for herpes simplex virus are heparan sulfate proteoglycans. *J. Cell Biol.* *116*, 1273–1281.
64. Compton, T., Nowlin, D.M., and Cooper, N.R. (1993). Initiation of human cytomegalovirus infection requires initial interaction with cell surface heparan sulfate. *Virology* *193*, 834–841.
65. DuBridge, R.B., Tang, P., Hsia, H.C., Leong, P.M., Miller, J.H., and Calos, M.P. (1987). Analysis of mutation in human cells by using an Epstein-Barr virus shuttle system. *Mol. Cell Biol.* *7*, 379–387.
66. Rasheed, S., Nelson-Rees, W.A., Toth, E.M., Arnstein, P., and Gardner, M.B. (1974). Characterization of a newly derived human sarcoma cell line (HT-1080). *Cancer* *33*, 1027–1033.
67. Schneider, U., Schwenk, H.U., and Bornkamm, G. (1977). Characterization of EBV-genome negative “null” and “T” cell lines derived from children with acute lymphoblastic leukemia and leukemic transformed non-Hodgkin lymphoma. *Int. J. Cancer* *19*, 621–626.
68. Tsuchiya, S., Yamabe, M., Yamaguchi, Y., Kobayashi, Y., Konno, T., and Tada, K. (1980). Establishment and characterization of a human acute monocytic leukemia cell line (THP-1). *Int. J. Cancer* *26*, 171–176.
69. Müllers, E., Stirnagel, K., Kaulfuss, S., and Lindemann, D. (2011). Prototype foamy virus gag nuclear localization: a novel pathway among retroviruses. *J. Virol.* *85*, 9276–9285.



70. Perkovic, M., Schmidt, S., Marino, D., Russell, R.A., Stauch, B., Hofmann, H., Kopietz, F., Kloke, B.P., Zielonka, J., Ströver, H., et al. (2009). Species-specific inhibition of APOBEC3C by the prototype foamy virus protein bet. *J. Biol. Chem.* 284, 5819–5826.
71. Duda, A., Stange, A., Lüftenecker, D., Stanke, N., Westphal, D., Pietschmann, T., Eastman, S.W., Linial, M.L., Rethwilm, A., and Lindemann, D. (2004). Prototype foamy virus envelope glycoprotein leader peptide processing is mediated by a furin-like cellular protease, but cleavage is not essential for viral infectivity. *J. Virol.* 78, 13865–13870.
72. Lüftenecker, D., Picard-Maureau, M., Stanke, N., Rethwilm, A., and Lindemann, D. (2005). Analysis and function of prototype foamy virus envelope N glycosylation. *J. Virol.* 79, 7664–7672.
73. Lindel, F., Dodt, C.R., Weidner, N., Noll, M., Bergemann, F., Behrendt, R., Fischer, S., Dietrich, J., Cartellieri, M., Hamann, M.V., and Lindemann, D. (2019). TraFo-CRISPR: enhanced genome engineering by transient foamy virus vector-mediated delivery of CRISPR/Cas9 components. *Mol. Ther. Nucleic Acids* 18, 708–726.
74. Swiersy, A., Wiek, C., Zentgraf, H., and Lindemann, D. (2013). Characterization and manipulation of foamy virus membrane interactions. *Cell Microbiol.* 15, 227–236.
75. Moebes, A., Enssle, J., Bieniasz, P.D., Heinkelein, M., Lindemann, D., Bock, M., McClure, M.O., and Rethwilm, A. (1997). Human foamy virus reverse transcription that occurs late in the viral replication cycle. *J. Virol.* 71, 7305–7311.
76. Mochizuki, H., Schwartz, J.P., Tanaka, K., Brady, R.O., and Reiser, J. (1998). High-titer human immunodeficiency virus type 1-based vector systems for gene delivery into nondividing cells. *J. Virol.* 72, 8873–8883.
77. Soneoka, Y., Cannon, P.M., Ramsdale, E.E., Griffiths, J.C., Romano, G., Kingsman, S.M., and Kingsman, A.J. (1995). A transient three-plasmid expression system for the production of high titer retroviral vectors. *Nucleic Acids Res.* 23, 628–633.
78. Lindemann, D., Stirrnagel, K., and Lüftenecker, D. (2013). Foamy Viral Envelope Genes (European Patent Office, Bulletin 2009/53), p. 55.
79. Vermeire, J., Naessens, E., Vanderstraeten, H., Landi, A., Iannucci, V., Van Nuffel, A., Taghon, T., Pizzato, M., and Verhasselt, B. (2012). Quantification of reverse transcriptase activity by real-time PCR as a fast and accurate method for titration of HIV, lenti- and retroviral vectors. *PLoS One* 7, e50859.
80. Dreier, J., Störmer, M., and Kleesiek, K. (2005). Use of bacteriophage MS2 as an internal control in viral reverse transcription-PCR assays. *J. Clin. Microbiol.* 43, 4551–4557.
81. Stange, A., Lüftenecker, D., Reh, J., Weissenhorn, W., and Lindemann, D. (2008). Subviral particle release determinants of prototype foamy virus. *J. Virol.* 82, 9858–9869.
82. Imrich, H., Heinkelein, M., Herchenröder, O., and Rethwilm, A. (2000). Primate foamy virus Pol proteins are imported into the nucleus. *J. Gen. Virol.* 81, 2941–2947.
83. Moreno-Mateos, M.A., Vejnar, C.E., Beaudoin, J.D., Fernandez, J.P., Mis, E.K., Khokha, M.K., and Giraldez, A.J. (2015). CRISPRscan: designing highly efficient sgRNAs for CRISPR-Cas9 targeting in vivo. *Nat. Methods* 12, 982–988.
84. Callahan, B.J., McMurdie, P.J., Rosen, M.J., Han, A.W., Johnson, A.J.A., and Holmes, S.P. (2016). DADA2: high-resolution sample inference from Illumina amplicon data. *Nat. Methods* 13, 581–583.